Geometrical analysis of spatio-temporal planning problems

Thesis by

Abhishek Tiwari

In Partial Fulfillment of the Requirements

for the Degree of

Doctor of Philosophy

California Institute of Technology

Pasadena, California

2007

(Defended Aug 29, 2006)

To my parents, Dr. Subodh Kumar Tiwari and Dr. Purnima Tiwari; my grandparents, Bhaskar Nath Tiwari, Maya Tiwari, Bipin Behari Mishra, and my dearest nani Kamla Mishra; and also my dear brother, Dr. Tanmay Tiwari

Acknowledgements

I would like to thank my advisor, Professor Richard Murray, from the bottom of my heart, for his continuing trust, support and encouragement throughout the period of my graduate studies at Caltech. Richard is the best supervisor I have had to date. I am truly impressed by his energy level and the way he motivates his students; he will always be my role model.

I would also like to thank Professor John Doyle, Professor Joel Burdick, Professor Babak Hassibi, and Dr. David Jeffcoat for agreeing to serve on my thesis defense committee.

My special thanks to Melvin Flores, Xin Liu, Alfredo Martinez, Stephen Prajna , Harish Bhat, Raktim Bhattacharya, Jimmy Fung, Ling Shi, Michael Epstein, Gloria Bain, and all other CDS students for making my stay in Steele a memorable experience.

My stay at Caltech was a lot of fun and it would not have been that way without my close friends Tejaswi Navilarekallu, Shankar Kalyanaraman, Krishnakanth Subramaniam, Sowmya Chandrashakher, Vijay Natraj, Amrit Pratap, Meher K. Ayalasomayajula, Vikram Deshpande, Swaminathan Krishnan, Subash Sukumara Pillai, and all the other OASIS friends.

Finally I would like to thank my parents and grandparents who have always emphasized the importance of education to me and my brother. Without their upbringing I would not have had the opportunity to earn a PhD from the prestigious California Institute of Technology.

Abstract

In this thesis I represent and analyze spatially and temporally constrained multi-agent planning problems using tools from geometry and advanced calculus. The two problems considered in this thesis are multi-agent rendezvous and dynamic sensor coverage. Together, these problems encompass the cooperation, constraint representation, and task scheduling aspects of multi-agent planning problems. I have represented the constraint of the rendezvous problem on the phase space and shown that the fulfilment of rendezvous constraints is equivalent to certain conical regions being invariant. Alternatively, for the dynamic coverage problem, the constraints can be adequately represented on the uncertainty space and sensor motion laws can be obtained by partitioning the uncertainty space and making decisions based on which partition the uncertainty lies in. I have examined convergence behavior of sensor motion under such laws.

Contents

List of Figures

List of Tables

Chapter 1

Introduction

All autonomous systems engineers and designers have to deal with planning problems. These problems arise in a variety of critical missions like spacecraft docking, Mars rovers, situational awareness, cooperative strike, cooperative exploration, missile interception, and robotic oceanography. Given a thorough understanding of multi-agent planning problems, one can envisage a lot of new applications where a transition from partial autonomy to complete autonomy is possible, for example border patrol, search and surveillance, cooperative UAV missions, weather monitoring, selective beam forming in radars, multi-agent consensus, load balancing, etc. Traditionally, planning has been studied as a subfield of artificial intelligence. Computer scientists and roboticists have modeled multi-agent plans using various approaches such as hybrid automata [1], petri nets [2], heuristics [3], Markov decision processes [4], and temporal logic for distributed decision making [5]. While control and network engineers usually start with a dynamical systems model of the agents and design cooperative control algorithms often in the presence of a non-ideal communication between agents [6], [7], [8], [9], and the reference therein. Due to the multitude of approaches available to solve planning problems, it becomes absolutely critical that there exist ways to quantify constraint satisfaction and analyze performance.

In this thesis, I present ideas that are based on geometry and calculus to illustrate constraint representation for two very different planning problems: multi-agent rendezvous and dynamic sensor coverage. The specific mathematical tools employed for the two problems may be different but the underlying philosophy is the same. Constraints are represented in the most appropriate space depending on the metric of performance for that particular

problem. Even though the tools employed here have been used in other fields of research, and the problems studied have been considered by other researchers, the demonstration of effective usage of geometric tools for analyzing the example planning problems is a novel contribution of this thesis.

While analyzing multi-agent planning, it is often desirable that there be methods to quantify, represent, and evaluate various important aspects of the problem. These aspects can be cooperation/coordination, task scheduling, spatio-temporal constraint representation, and fault tolerance. If one is further interested in synthesis of algorithms to solve these problems, the choice of an appropriate metric also becomes important. The two example problems that I will deal with in this thesis relate to cooperation/coordination and multi-task scheduling. Cooperation and coordination are central to and very critical in multi-agent rendezvous missions, while task scheduling can be viewed as an equivalent problem to dynamic sensor coverage. For both these problems I will identify the adequate space to represent the constraints and the right geometric tools to deal with them. For both these problems spatio-temporal constraints are represented in a manner specific to the problem. I will not consider the fault tolerance aspect of multi-agent planning in this thesis.

Multi-agent rendezvous is the problem of designing control laws for multiple heterogenous agents in order for them to converge to a common location at the same time. It is absolutely critical in certain applications of the rendezvous problem that all the agents reach the rendezvous location within a short time interval of each other. Cooperative strike is such an application, where failure to meet this constraint may cause early detection and may possibly result in aborting the mission. In this thesis I represent this cooperation/coordination constraint on the phase space using the idea of cone invariance and stability.

Chapters 2 and 3 deal with the rendezvous problem. In Chapter 2, I present a dynamical systems representation for multi-agent rendezvous on the phase plane. I restrict my attention to two agents, each with scalar dynamics. The problem of rendezvous is cast as a stabilization problem, with a set of constraints on the trajectories of the agents, defined on the phase plane. I also describe a method to generate control Lyapunov functions that, when used in conjunction with a stabilizing control law, such as Sontag's formula, makes sure that the two-agent system attains rendezvous. The main result of this chapter is a

Lyapunov-like certificate theorem that describes a set of constraints, which when satisfied are sufficient to guarantee rendezvous.

In Chapter 3, I pose the N scalar-agent rendezvous as a polyhedral cone invariance problem in the N-dimensional phase space. The underlying dynamics of the agents are assumed to be linear. I derive a condition for positive invariance for polyhedral cones. Based on this condition, I demonstrate that the problem of determining a certificate for rendezvous can be stated as a convex feasibility problem. Under certain rendezvous requirements, I show that there are no robust closed-loop linear solutions that satisfy the invariance conditions. I show that the treatment of the rendezvous problem on the phase plane can be extended to the case where agent dynamics are non-scalar.

The second part of my thesis deals with the dynamic sensor coverage problem. It is an example multi-agent planning problem where I highlight the task scheduling aspect. The objective here is to keep track of the values of a few uncertain parameters in a dynamic environment. Imagine there are only a few limited range sensors available to accomplish this task, but these sensors are mobile. Now the problem is to determine what is the best way to move these sensors around so as to collect the maximum possible information about the environment or, in other words, keep the overall uncertainty of the environment bounded. If one throws out the path planning part of the sensor coverage problem, this problem turns out to be equivalent to the sensor scheduling and load balancing problems. For the dynamic sensor coverage problem, since the appropriate metric is the error covariance of parameters at different locations, the analysis is best captured on the uncertainty space. I partition the uncertainty space into different regions and take sensor motion decisions based on where the relative uncertainty at a given time lies. In this thesis I also present analysis of a couple of stochastic sensor motion algorithms for the dynamic sensor coverage problem.

This problem is covered in Chapters 4 and 5. In Chapter 4, I introduce a theoretical framework for the dynamic sensor coverage problem for the case with multiple discrete time linear stochastic systems placed at different spatial locations. The objective is to keep an appreciable estimate of the states of the systems at all times by deploying a few limited range mobile sensors. The sensors implement a Kalman filter to estimate the states of all the systems. In this chapter I present results for a single sensor executing two different

random motion strategies. Under the first strategy the sensor motion is an independent and identically distributed random process and a discrete time, discrete state ergodic Markov chain under the second strategy. For both these strategies I give conditions under which a single sensor fails or succeeds to solve the dynamic coverage problem. I also demonstrate that the conditions for the first strategy are a special case of the main result for the second strategy.

In Chapter 5, I present an analysis of the dynamic sensor coverage problem with uncertainty feedback. I consider a simple case of two spatially separate uncertain systems **1** and **2**. Contrary to Chapter 4, I take a deterministic approach in this chapter; the sensor decides to measure system **1** or **2** based on the relative uncertainty of its estimates of the states of the two systems. Error covariance is used as a metric for uncertainty of estimates. Based on the sensor measurements, the error covariance evolves according to the Lyapunov or the Riccati map. The uncertainty space is partitioned and each partition has a different sensor motion decision associated with it. For a certain class of partitions I prove the existence and local stability of a unique periodic steady state orbit. I prove global stability for a scalar special case. I also show by way of an example that by changing certain parameters in these partitions stable orbits of higher periods can be obtained. Implications of this work and comparisons with existing work in the sensor scheduling and sensor coverage literature are also presented. In the end I present a discussion on future extensions of this work. I demonstrate the utility of uncertainty feedback over open loop algorithms for an example with time varying systems. Simulation examples are provided to illustrate the main concepts.

Chapter 2

Lyapunov certificates for scalar rendezvous

2.1 Introduction

Recently there has been considerable interest in multi-agent coordination or cooperative control (as cited in [10] and [11] for instance). This has led to the emergence of several interesting control problems. One such problem is the *rendezvous problem*. In a rendezvous problem, one desires to have several agents arrive at predefined destination points simultaneously. Cooperative strike or cooperative jamming are two examples of the rendezvous problem. In the first scenario, multiple strikes are executed *within an interval*, from different agents firing from different distances and traveling at different speeds. In the second scenario, one or more agents need to start jamming *slightly before* the strike vehicle enters the danger zone and sustain jamming until strike vehicle exits. In both the scenarios, it is imperative that all the agents act simultaneously else the objective is not fulfilled.

The idea of rendezvous extends beyond just convergence to a static set of destination points or the origin. The tools we develop for rendezvous can also be applied to formation flying or interception problems with small modifications. Interception of incoming ballistic missiles is a rendezvous problem where the origin becomes a moving target. However, interception problems are different as the agents involved are non-cooperative. Formation flying is a type of rendezvous problem where multiple agents must coordinate position and velocity. The docking of two spacecraft is a rendezvous problem that involves the

two spacecraft matching both position and velocity with the proper orientation. Air-to-air refueling is another rendezvous problem. Additional applications arise in submersibles where robotic vehicles must converge upon a set location, either moving or stationary.

As the push towards unmanned vehicles becomes more prevalent in the aerospace industry, methods for guaranteeing rendezvous will be necessary. It will be necessary to answer whether a mission in a cooperative control framework can be accomplished with a high degree of confidence in the presence of uncertainties. The uncertainty set can include differing flight conditions, local parametric variations, component failures on an aircraft, and communications variability such as loss of packets, temporary loss of link, etc.

In the existing literature, several researchers have addressed problems related to path planning with timing constraints. In 1963, Meschler in [12] investigated a time optimal rendezvous problem for linear time varying systems. He assumed that both the rendezvous point and rendezvous time are not known a priori and that determining the minimum time at which rendezvous occurred was of interest. In principle, complicated rendezvous problems can be formulated using optimal control theory [13] and solved numerically. However, for many vehicles, obstacles, and threats, the resulting optimization problem becomes quite complicated and the computational time increases very rapidly with problem size. In [14], [8] McLain et al. have proposed decomposition methods that break down the monolithic problem into subproblems that can be solved efficiently in a decentralized manner. Similar decomposition methods have also being proposed in [9] and [15] that solve path planning problems with timing constraints in a decentralized manner. Heuristic search-based algorithms have also been proposed as an alternative that approximates single large scale optimization problems into decoupled, partially distributed problems enabling faster computation [16],[17].

In this chapter we approach the rendezvous problem from the point of view of Lyapunov stability [18]. Örgen et al. in [19] have recently proposed a Lyapunov function approach to multi-agent coordination with application to formation flying. In this chapter, we propose Lyapunov function approach to the rendezvous problem.

The chapter is organized as follows: The rendezvous problem is defined in Section 2.2 along with notions of perfect and approximate rendezvous and with an interpretation of ren-

dezvous on the phase plane. An example is given in Section 2.3 of a system of agents that achieve rendezvous under certain conditions with a Lyapunov-function-based controller. A level-set method for constructing Lyapunov functions for use in rendezvous control is given in Section 2.4. The subject of rendezvous certificates is addressed in Section 2.5, and a certificate theorem is given for guaranteeing rendezvous using a certain class of Lyapunov functions. An example illustrating the use of this certificate theorem is given, and remarks are made concerning this and future work.

The results presented in this chapter have been published in [20].

2.2 The rendezvous problem

In this chapter we define the rendezvous problem to be the problem of determining a control algorithm that drives multiple agents to a desired destination point. The trajectories must be such that the agents visit the destination point only once and arrive at the same time. We present results for two agents with scalar dynamics.

Consider two scalar systems or agents $\mathcal{V}_1$ and $\mathcal{V}_2$ defined as

$$\begin{aligned} \mathcal{V}_1 &: \quad \dot{x}_1 = f_1(x_1) + g_1(x_1)u_1\,; \quad f_1(0) = 0, \\ \mathcal{V}_2 &: \quad \dot{x}_2 = f_2(x_2) + g_2(x_2)u_2\,; \quad f_2(0) = 0, \end{aligned} \tag{2.1}$$

where $x_i \in \mathbb{R}$ for $i \in \{1, 2\}$ and the destination point being the origin. Let x_1 and x_2 in eqn. (2.1) be the spatial coordinates of $\mathcal{V}_1$ and $\mathcal{V}_2$ on the real line. It is of interest to design control laws u_1 and u_2 such that $\mathcal{V}_1$ and $\mathcal{V}_2$ reach the origin of the real line at the same time. This is depicted in fig. 2.1(a).

Clearly agents that are exponentially stable will reach the origin as time tends to infinity. Thus comparison of arrival times at the origin, of two different agents becomes meaningless. Even with cooperative control in place, if the origin is exponentially stable, rendezvous at the origin will occur at infinite time in theory. From a practical standpoint, it is desired that the agents achieve rendezvous in finite time. For this reason we relax the definition of rendezvous to be such that rendezvous is achieved if the agents enter a certain neighborhood around the origin, at the same time. We define this region to be the

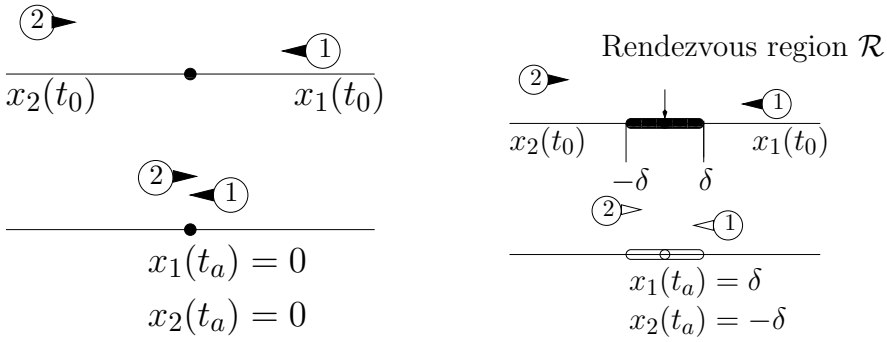

(a) At the origin (b) At the rendezvous region $\mathcal{R}$

Figure 2.1: Rendezvous on the real line.

rendezvous region $\mathcal{R}$:

$$\mathcal{R} = \{x \in \mathbb{R} : -\delta \leq x \leq \delta\} \text{ for some } \delta > 0$$

Therefore a valid rendezvous is one in which agents enter $\mathcal{R}$ at the same time. This is illustrated in fig. 2.1(b). In Section 2.2.2 we will relax this definition for agents entering $\mathcal{R}$ at approximately the same time.

2.2.1 Rendezvous interpretation on phase plane

Rendezvous is best visualized on the phase plane. To interpret rendezvous for the scalar systems in eqn. (2.1) in the phase plane, we define the following:

$$\begin{aligned} U_1 &= \{(x_1, x_2) : -\delta \leq x_1 \leq \delta\}, \\ U_2 &= \{(x_1, x_2) : -\delta \leq x_2 \leq \delta\}, \\ \mathcal{S} &= U_1 \cap U_2, \\ \mathcal{F} &= (U_1 \cup U_2) - (U_1 \cap U_2), \\ \mathcal{W} &= (\mathbb{R}^2 - (U_1 \cup U_2)). \end{aligned} \tag{2.2}$$

We refer to $\mathcal{S}$ as the *rendezvous square* and $\mathcal{F}$ as the *forbidden region*.

With reference to fig. 2.2(a), the strip on the x_2-axis is U_1, the strip on the x_1-axis is the region U_2, and the rendezvous square is the destination set where the trajectories must converge. The rendezvous square $\mathcal{S}$ is the set of configurations with both agents in the

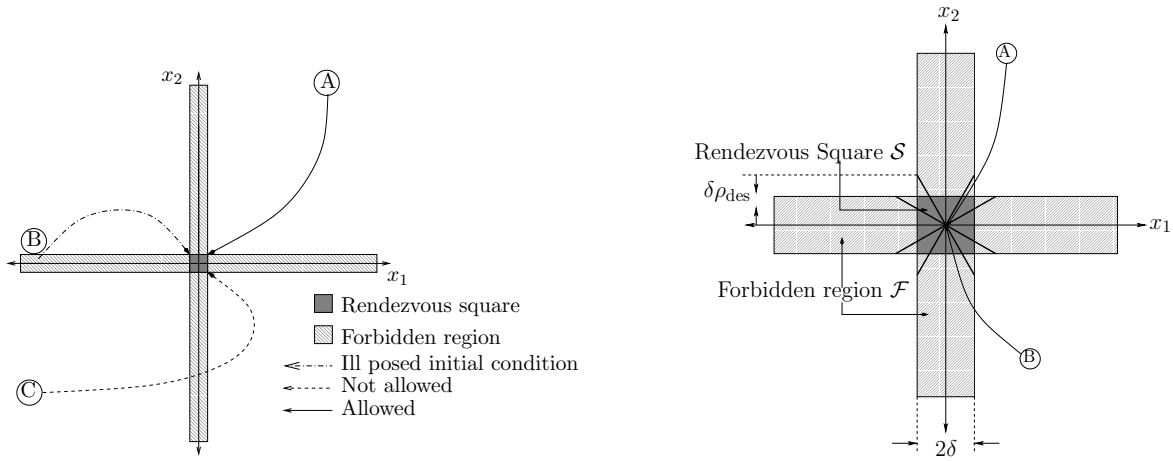

(a) Rendezvous in phase plane

(b) Approximate Rendezvous in phase plane

Figure 2.2: Rendezvous illustration

rendezvous region $\mathcal{R}$. The rendezvous problem is well posed if the initial conditions of the two agents satisfy

$$(x_1(0), x_2(0)) \in \mathcal{W}, \tag{2.3}$$

i.e., both the agents start outside the rendezvous region. If the condition in eqn. (2.3) is violated, either $\mathcal{V}_1$, $\mathcal{V}_2$, or both start from within the rendezvous region $\mathcal{R}$. In fig. 2.2(a) trajectory B starts from an invalid initial point.

The forbidden region is the set of points $\mathcal{F}$ where one agent enters the rendezvous region much before the other. In fig. 2.2(a), trajectory C crosses the forbidden region, which implies that agent $\mathcal{V}_1$ with state x_1 comes within the rendezvous region prior to the final entry. Such trajectories are not acceptable, i.e., the trajectories must satisfy

$$(x_1(t), x_2(t)) \notin \mathcal{F} \quad \forall t. \tag{2.4}$$

Trajectory A is an example of two agents, with valid initial conditions, achieving rendezvous as desired.

2.2.2 Perfect and approximate rendezvous

With the constraint defined in eqn. (2.4), the only way trajectories can enter $\mathcal{S}$ is through the corners of the rendezvous square, i.e., through one of the points

$$(\delta, \delta), (\delta, -\delta), (-\delta, \delta), \text{ and } (-\delta, -\delta).$$

This implies that the agents are constrained to enter $\mathcal{S}$ at precisely the same time, which is the time the trajectory meets one of the four corners of $\mathcal{S}$ in the phase plane. In reality, agents $\mathcal{V}_1$ and $\mathcal{V}_2$ may reach the rendezvous region within ΔT seconds of each other (through the forbidden region, as is shown below). We now refer to the case when ΔT is zero as *ideal* or *perfect* rendezvous and the case when ΔT is small as *real* or *approximate* rendezvous.

Since the phase plane does not reveal time explicitly, we use a related measure ρ to characterize rendezvous. We will first define ρ; its relation to ΔT will be explained thereafter. To define ρ, we first introduce $t_{\mathcal{V}_1}$ and $t_{\mathcal{V}_2}$ as the arrival times of agents $\mathcal{V}_1$ and $\mathcal{V}_2$ at the boundary of the rendezvous region $\mathcal{R}$, i.e.,

$$\begin{aligned} t_{\mathcal{V}_1} &= \min\ [\ t \mid x_1(t) \in U_1\ ] \\ t_{\mathcal{V}_2} &= \min\ [\ t \mid x_2(t) \in U_2\ ]. \end{aligned}$$

Clearly, ΔT is given by

$$\Delta T = \left| t_{\mathcal{V}_1} - t_{\mathcal{V}_2} \right|. \tag{2.5}$$

Therefore, the time t_a at which the trajectory enters region $U_1 \cup U_2$ in the phase plane is given by

$$t_a = \min(t_{a_1}, t_{a_2}).$$

For a given trajectory ($x(t) = [x_1(t)\ x_2(t)]^T$), ρ is the maximum ratio of the distance from the origin of the two agents, after one of them has reached the rendezvous region $\mathcal{R}$. It can be expressed as

$$\rho = \frac{\max(|x_1(t_a)|, |x_2(t_a)|)}{\min(|x_1(t_a)|, |x_2(t_a)|)} = \frac{\max(|x_1(t_a)|, |x_2(t_a)|)}{\delta}. \tag{2.6}$$

For the rest of the chapter, rendezvous will always be specified by δ and a design measure of approximate rendezvous, ρ_{des}. In other words we will call a given rendezvous successful, if all the trajectories satisfy

$$\rho \ \leq \ \rho_{\text{des}}. \tag{2.7}$$

This notion of approximate rendezvous is illustrated in fig. 2.2(b). Whenever a trajectory starting in the first quadrant enters region $U_1 \cup U_2$ it is constrained to lie within the angle generated by joining the points

$$(\delta, \delta\rho_{\text{des}}),\ (0,0),\ \text{and}\ \ (\delta\rho_{\text{des}}, \delta)\,.$$

There exist similar constraints for trajectories originating in the other quadrants. The introduction of ρ in the definition of rendezvous allows trajectories to enter forbidden region $\mathcal{F}$ as long as they remain within the above mentioned angle set by the design constraint.

By the definition of ρ in eqn. (2.6) it is clear that for a given trajectory $\rho \geq 1$. Therefore, a specification of rendezvous is meaningful if and only if

$$\rho_{\text{des}} \geq 1. \tag{2.8}$$

Note that for perfect rendezvous the specification becomes $\rho_{\text{des}} = 1$.

In the worst case, at the time of entry of the first agent, t_a, the distances of the two agents from the origin can differ by $\delta(\rho_{\text{des}} - 1)$. By ensuring that the trajectories remain within the bold lines in fig. 2.2(b), upon entry in region $U_1 \cup U_2$ we can make sure that the two agents enter rendezvous region $\mathcal{R}$ within a small time ΔT of each other. Thus the constraint in eqn. (2.7) helps keep ΔT small.

In fig. 2.2(b) both trajectories A and B fail to achieve perfect rendezvous as they do not enter the rendezvous square $\mathcal{S}$ from its four corners. On the basis of eqn. (2.7), trajectory B is unacceptable. Trajectory A is acceptable since it lies within the angle defined by the bold lines.

2.3 Rendezvous using control lyapunov functions

In this section we motivate the use of control Lyapunov functions (CLFs) to solve the rendezvous problem. Consider the Lyapunov function candidate

$$V(x_1, x_2) = x_1^2 + x_2^2 + (x_1^2 - x_2^2)^2. \tag{2.9}$$

Ensuring $\dot{V} < 0$ guarantees that all the three terms in eqn. (2.9) go to zero as time tends to infinity. If x_1 and x_2 denote the spatial coordinates of agents $\mathcal{V}_1$ and $\mathcal{V}_2$ and the origin is the rendezvous point, the first two terms ensure that they converge to the origin and the third term ensures that the agents reach the origin simultaneously. This is demonstrated by the following example:

Let the dynamics of the agents be given by

$$\begin{aligned} \dot{x}_1 &= u_1 \\ \dot{x}_2 &= u_2. \end{aligned} \tag{2.10}$$

It is easy to verify that $V(x)$ in eqn. (2.9) is a CLF. Sontag in [21] proposed a formula for producing a stabilizing controller based on the existence of a CLF $V(x)$. Because of its guarantee of stabilization and of providing a convenient relationship between closed-loop trajectories and CLF level sets, Sontag's formula is used here. For non-linear systems with affine input such as

$$\dot{x} = f(x) + g(x)u,$$

Sontag's formula can be written as

$$u_s = \begin{cases} -\frac{V_x f + \sqrt{(V_x f)^2 + q(x) V_x g g^T V_x^T}}{V_x g g^T V_x^T} g^T V_x^T & V_x g \neq 0, \\ 0 & V_x g = 0 \end{cases} \tag{2.11}$$

where $V_x = \frac{\partial V(x)}{\partial x}$.

For the system in eqn. (2.10) and control derived from $V(x)$ in eqn. (2.9) using Sontag's

formula, the phase portrait is shown in fig. 2.3(a). The term $(x_1^2 - x_2^2)^2$ in eqn. (2.9) ensures

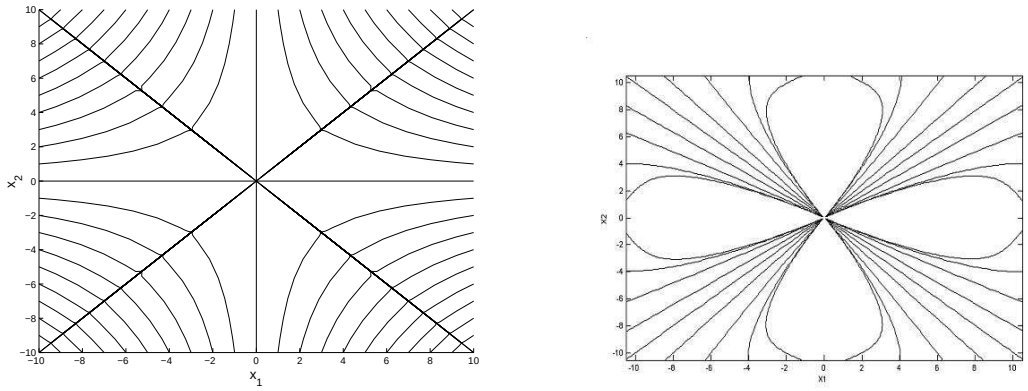

(a) (b)

Figure 2.3: Rendezvous using control Lyapunov functions.

that the agents become equidistant from the origin by converging to the lines $x_1 = \pm x_2$ prior to their arrival at the origin. In this sense, rendezvous is achieved for any ρ_{des} for any δ. Fig. 2.3(b) shows the phase portrait for the same system but with Lyapunov function defined as

$$V(x_1, x_2) = (x_1^2 + x_2^2)\left[a + be^{-8x_1^2x_2^2/d^2(x_1^2+x_2^2)^2}\right]. \tag{2.12}$$

I will present the motivation behind choosing the above Lyapunov function in the next section. Rendezvous is achieved by $\mathcal{V}_1$ and $\mathcal{V}_2$ in fig. 2.3(b) only under restricted values of ρ_{des} for a given δ. In one sense, however, rendezvous achieved by $\mathcal{V}_1$ and $\mathcal{V}_2$ in fig. 2.3(b) is 'better' than that in fig. 2.3(a) because the agents are equidistant from the origin only locally. Rendezvous in fig. 2.3(a) forces the agents to be equidistant from the origin even at large distances, which may not be necessary.

Thus, it is possible to implicitly satisfy the constraints on ρ, as defined in eqn. (2.7), if the Lyapunov function has a certain form. For valid rendezvous, trajectories in the phase plane should not cross either axis. If $\dot{V}$ is negative definite for all points in the phase plane and trajectories are constrained to be within the quadrant they start from, outside $\mathcal{S}$, the level sets are expected to have a clover leaf appearance as shown in fig. 2.4(b). Figure 2.4(b) shows the level sets of the Lyapunov function defined in eqn. (2.12). The level set of these control Lyapunov functions provides insight into why rendezvous is achieved for

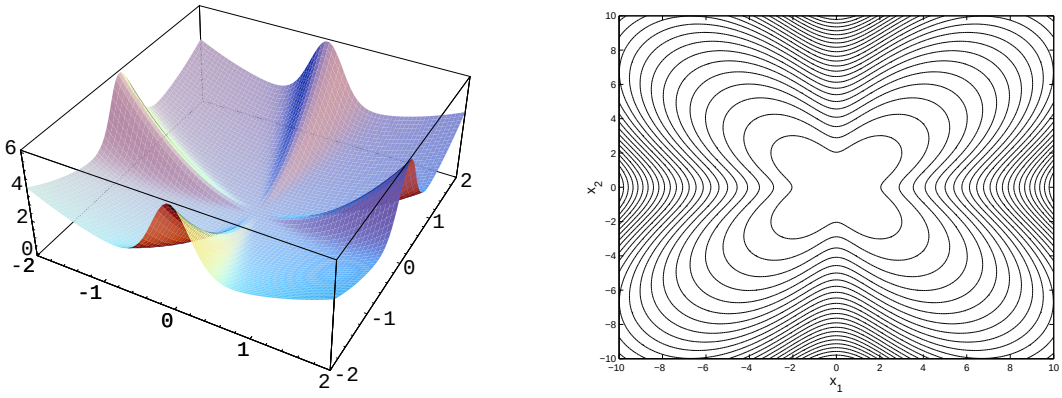

(a) (b)

Figure 2.4: Desired Lyapunov surface and its level sets.

these cases. With control using Sontag's formula for the system in eqn. (2.10), rendezvous is achievable because trajectories are constrained to be normal to the level set contours. Controllers based on CLFs, whose level sets are similar to those in fig. 2.4(b), should drive agents for system eqn. (2.10) to a successful rendezvous. The next section describes a level set method for constructing control Lyapunov functions, and a certificate theorem for testing whether rendezvous is achievable for a system is given in Section 2.5.

2.4 Generating lyapunov surfaces using level sets

In this section we will present a method to design Lyapunov surfaces by first designing their level sets. As already demonstrated in the previous section, the level sets for all the cases we are interested in look similar to that shown in fig. 2.4(b)

The main idea is to first write down an equation for a curve in $\mathbb{R}^2$ using polar coordinates $r^n = h(\theta), n \in \mathbb{Z}^+$. Then we try to find a positive definite function $V(r, \theta)$ such that for some $c_0 > 0$, the following two equations are equivalent:

$$V(r, \theta) = c_0, \tag{2.13}$$

$$r^n = h(\theta), n \in \mathbb{Z}^+; \tag{2.14}$$

i.e., they describe the same curve in $\mathbb{R}^2$.

Definition 2.4.1. *We define a family $\mathcal{T}$ of real valued functions $h : [0, 2\pi] \to \mathbb{R}$ with the following properties:*

1. *the function h is continuous and strictly differentiable;*
2. *the function h is strictly positive:*

$$h(\theta) > 0, \quad \forall \quad \theta;$$

3. *in the interval $\theta \in [0, \pi/2)$, h attains a minimum value at $\theta = 0$;*
4. *In the interval $\theta \in [0, \pi/2)$, h attains a maximum value at $\theta = \pi/4$;*
5. *the function h is symmetric about $\theta = \pi/4$:*

$$h(\theta) = h(\pi/2 - \theta); \text{ and}$$

6. *the function h is periodic with period $\pi/2$:*

$$h(\theta) = h(\pi/2 + \theta).$$

Example 1. *The function*

$$h(\theta) = \frac{\alpha + \beta}{2} - \frac{\alpha - \beta}{2}\cos(4\theta), \ \forall \alpha, \beta > 0 \text{ and } \alpha > \beta$$

satisfies all the properties in Definition (2.4.1). The fig. 2.5(a) shows a plot of $h(\theta)$ vs θ for $\alpha = 5$ and $\beta = 1$.

Example 2. *The function*

$$h(\theta) = \frac{1}{a + be^{-\frac{1-\cos 4\theta}{d^2}}},$$

where a, b, d $\in \mathbb{R}$ and

$$a + b > 0$$

is also a member of $\mathcal{T}$.

Definition 2.4.2. *We define a family C of closed curves $c(r, \theta) = 0$ in $\mathbb{R}^2$, where*

$$c(r, \theta) = 0 \text{ and } r^n = h(\theta)$$

describe the same closed curve in $\mathbb{R}^2$ for $h(\theta) \in \mathcal{T}$ and a real number $n > 1$, with $\mathcal{T}$ as defined above.

Example 3. *The closed curve described by*

$$r^2 = 3 - 2\cos(4\theta)$$

is a member of C as defined above. See fig. 2.5(b)

Example 4. *The closed curve described by*

$$r^2 = \frac{1}{a + be^{-\frac{1-cos4\theta}{d^2}}}$$

belongs to the family C of closed curves as defined above.

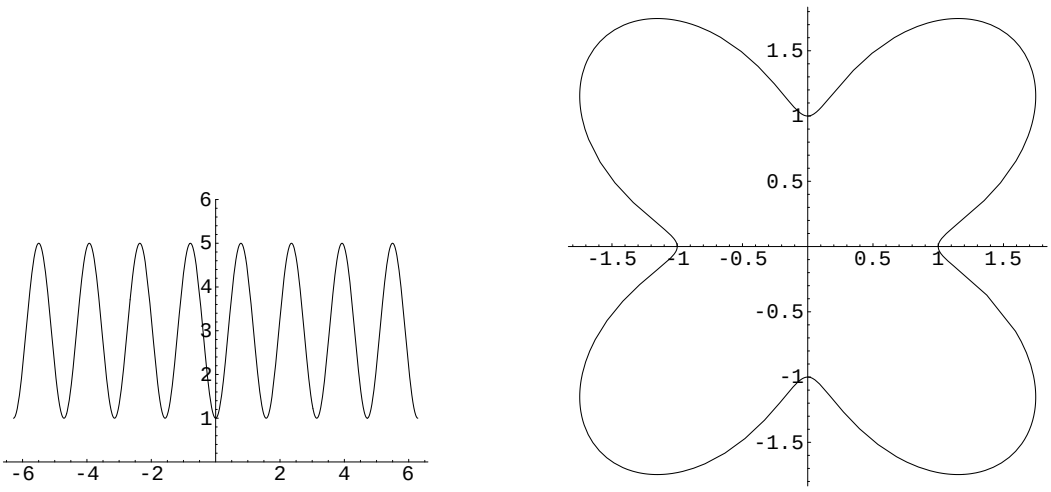

(a) $h(\theta)$ (b) Cloverleaf appearance

Figure 2.5: Examples.

Note that the properties of the function $h(\theta) \in \mathcal{T}$ presented in Definition 2.4.1 gives it the cloverleaf appearance, as shown in fig. 2.5(b).

Constructing a Lyapunov surface. We can now construct a Lyapunov surface as

$$V(r,\theta) = \frac{c_0 r^n}{h(\theta)}, \quad c_0 > 0, \quad h(\theta) \in \mathcal{T}, \quad n \in \mathbb{R}, \quad n > 1. \tag{2.15}$$

The following is a lemma for the properties of the associated Lyapunov function to the surface mentioned above. A proof is listed only for part 5 of the lemma.

Lemma 2.4.1. The Lyapunov surface $V(r,\theta)$ of eqn. (2.15) has the following properties:

1. $V(r,\theta)$ is continuous and differentiable everywhere on $\mathbb{R}^2$;
2. at the origin of $\mathbb{R}^2$
$$V(0,\theta) = 0;$$
3. $V(r,\theta)$ is positive definite:
$$V(r,\theta) > 0, \quad \forall\theta, \quad r > 0;$$
4. all level curves of $V(r,\theta)$ belong to the family C of curves as defined above; and
5. all the level curves $V(r,\theta) = \xi$ have the same slope $\frac{dy}{dx}$ at the point of intersection with any line $\theta = \theta_0$ irrespective of the value of ξ.

Proof of property 5 of Lemma 2.4.1: Consider a level curve of $V(r,\theta)$:

$$\frac{c_0 r^n}{h(\theta)} = \xi, \quad \xi > 0 \tag{2.16}$$

Now for any curve in $\mathbb{R}^2$

$$\frac{dy}{dx} = \frac{\frac{dr}{d\theta}\sin\theta + r\cos\theta}{\frac{dr}{d\theta}\cos\theta - r\sin\theta}, \tag{2.17}$$

the point of intersection of the curve (2.16) with the line $\theta = \theta_0$ is given by

$$\left(\left[\frac{\xi h(\theta_0)}{c_0}\right]^{1/n}, \theta_0\right). \tag{2.18}$$

The quantity $\frac{dr}{d\theta}$ can be evaluated as

$$\frac{dr}{d\theta} = \frac{\xi}{c_0}\frac{h'(\theta)}{nr^{n-1}}. \tag{2.19}$$

Therefore, the slope evaluated at the point of intersection is given by

$$\left.\frac{dy}{dx}\right|_{\left(\left[\frac{\xi h(\theta_0)}{c_0}\right]^{1/n},\theta_0\right)} = \frac{h'(\theta_0)\sin\theta_0 + nh(\theta_0)\cos\theta_0}{h'(\theta_0)\cos\theta_0 - nh(\theta_0)\sin\theta_0}, \tag{2.20}$$

which is independent of ξ.

□

Example 5. *The Lyapunov surface in eqn. (2.12) in Section 2.3 can be generated by using the function $h(\theta)$ as given in Example 2 and eqn. (2.15) with $n = 2$ and $c_0 = 1$ and then converting to Cartesian coordinates.*

2.5 Rendezvous certificates

In Section 2.3 we listed an example of a controller for achieving rendezvous. In this section we present a Lyapunov certificate theorem for rendezvous. Schemes for guaranteeing rendezvous are absolutely necessary to answer whether a mission in a cooperative control framework can be accomplished with a high degree of confidence in the presence of uncertainties. The uncertainty set can include differing flight conditions, local parametric variations, component failures on an aircraft, and communications variability such as loss of packets, temporary loss of link, etc. The result presented here is only a sufficient condition.

Consider the following system of two agents:

$$\begin{aligned} \mathcal{V}_1 &: \quad \dot{x}_1 = f_1(x_1, x_2)\,; \quad f_1(0,0) = 0, \\ \mathcal{V}_2 &: \quad \dot{x}_2 = f_2(x_1, x_2)\,; \quad f_2(0,0) = 0, \end{aligned} \tag{2.21}$$

where x_1 and $x_2 \in \mathbb{R}$. The problem is to determine whether or not $\mathcal{V}_1$ and $\mathcal{V}_2$ achieve

rendezvous in the region $\mathcal{R}$ around the origin given a specification ρ_{des} as defined in Section 2.2.2. Before we state our main result we give a few definitions and a lemma.

Definition 2.5.1. *Coverage Angle: We define the* coverage angle θ_0 *as*

$$\theta_0 = \tan^{-1}\left(\frac{1}{\rho_{des}}\right). \tag{2.22}$$

Since we know from eqn. (2.8) that

$$\rho_{des} \geq 1,$$

therefore

$$\theta_0 \in [0, \pi/4]. \tag{2.23}$$

Definition 2.5.2. *We define the region $\mathcal{I} \subset \mathbb{R}^2$ in polar coordinates as*

$$\mathcal{I} = \{(r,\theta) | \ \frac{n\pi}{2} + \theta_0 \leq \theta \leq \frac{(n+1)\pi}{2} - \theta_0, \quad n \in \mathbb{Z}\}. \tag{2.24}$$

The region $\mathcal{I}$ is shown in fig. 2.6.

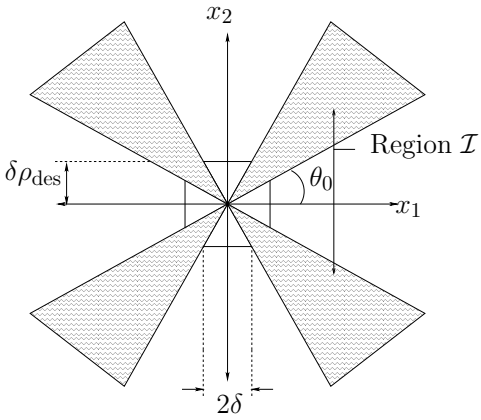

Figure 2.6: The region $\mathcal{I}$.

Definition 2.5.3. *Define region $\mathcal{Z} \subset \mathbb{R}^2$ as*

$$\mathcal{Z} = \mathcal{I} \cap \mathcal{W}, \tag{2.25}$$

where $\mathcal{W}$ is given by eqn. (2.2).

Note that, by this definition, trajectories in $\mathcal{Z}$ also fall within the specification ρ_{des} and are thus considered valid for rendezvous. However, trajectories with initial conditions in $\mathcal{Z}$ may not stay in $\mathcal{Z}$. The following is a lemma for the invariance of $\mathcal{I}$ (and thus $\mathcal{Z}$) given a Lyapunov function of the form described in the previous section:

Lemma 2.5.1 (Invariance of region $\mathcal{I}$)**.** Consider a system of two agents

$$\begin{aligned} \mathcal{V}_1 \ : \quad \dot{x}_1 &= f_1(x_1, x_2)\,; \quad f_1(0,0) = 0 \\ \mathcal{V}_2 \ : \quad \dot{x}_2 &= f_2(x_1, x_2)\,; \quad f_2(0,0) = 0 \end{aligned}$$

where x_1 and $x_2 \in \mathbb{R}$, and suppose that the origin is shown to be asymptotically stable under a Lyapunov function of the form

$$V(x_1, x_2) = \frac{c_0({x_1}^2 + {x_2}^2)^{n/2}}{h\left(\tan^{-1}\left(\frac{x_2}{x_1}\right)\right)}$$

with positive real constants c_0 and $n \geq 1$, and with $h \in \mathcal{T}$. Furthermore, consider a coverage angle θ_0 corresponding to a design specification ρ_{des} and identified with regions $\mathcal{I}$ and $\mathcal{Z}$. The region $\mathcal{I}$ is an invariant region for the system if

$$\left.\frac{(\frac{\partial V}{\partial x})^T . f(x_1, x_2)}{\left\|\frac{\partial V}{\partial x}\right\| \|f(x_1, x_2)\|}\right|_{x_2 = x_1 \tan\theta_0} \leq \cos(\pi + \theta_1 - \theta_0), \tag{2.26}$$

where

$$\begin{aligned} f(x_1, x_2)^T &= [f_1(x_1, x_2) \quad f_1(x_1, x_2)] \\ \tfrac{\partial V}{\partial x}^T &= \left[\tfrac{\partial V}{\partial x_1} \quad \tfrac{\partial V}{\partial x_2}\right] \end{aligned}$$

with

$$\theta_1 = \tan^{-1}\left(\frac{h'(\theta_0)\sin\theta_0 + nh(\theta_0)\cos\theta_0}{h'(\theta_0)\cos\theta_0 - nh(\theta_0)\sin\theta_0}\right), \text{ and } \theta_1 \geq \theta_0.$$

Note that θ_1 is defined along the boundary of $\mathcal{I}$ with $\theta_1 \geq \theta_0$. Conceptually, invariance is determined from the inner product of the closed-loop vector field f along the boundary of $\mathcal{I}$ and the boundary itself. This lemma follows from examining the geometry of the boundary of the region $\mathcal{I}$, the level set curves of the Lyapunov function V, and the trajectory as we will now see in the proof.

Proof of Lemma 2.5.1: Suppose that the origin of the system

$$\begin{aligned} \mathcal{V}_1 &: \quad \dot{x}_1 = f_1(x_1, x_2); \quad f_1(0,0) = 0 \\ \mathcal{V}_2 &: \quad \dot{x}_2 = f_2(x_1, x_2); \quad f_2(0,0) = 0 \end{aligned}$$

is asymptotically stable under the Lyapunov function

$$V(x_1, x_2) = \frac{c_0({x_1}^2 + {x_2}^2)^{n/2}}{h\left(\tan^{-1}\left(\frac{x_2}{x_1}\right)\right)}.$$

A proof will be constructed by contradiction.

We first assume the contradictory and say that a particular trajectory of the system (2.21)

$$x(t): \quad t \in [t_i, t_f] \tag{2.27}$$

with $x(t_i) \in \mathcal{Z}$ goes out of the region $\mathcal{I}$, i.e.

$$x(t_f) \notin \mathcal{I}. \tag{2.28}$$

Now since the trajectory is continuous there exists $t_c > t_i$ such that

$$x(t_c) \in \sigma(\mathcal{I}) \tag{2.29}$$

where $\sigma(\mathcal{I})$ denotes the boundary of the region $\mathcal{I}$.

Since $h(\theta) \in \mathcal{T}$ it is periodic with period $\pi/2$ and is symmetric about $\theta = \pi/4$, we can without loss of generality assume that $x(t_c)$ lies on the line $\theta = \theta_0$. Because of the periodic and symmetric nature of $h(\theta)$ a similar proof, like the one about to be presented will hold if $x(t_c)$ lies on any other line bounding region $\mathcal{I}$.

Since t_c is the time, the trajectory crosses over from region $\mathcal{I}$ to region $\mathbb{R}^2 - \mathcal{I}$, therefore

$$\begin{aligned} x(t_c^-) &\in \mathcal{I} \\ x(t_c^+) &\in \mathbb{R}^2 - \mathcal{I}. \end{aligned} \tag{2.30}$$

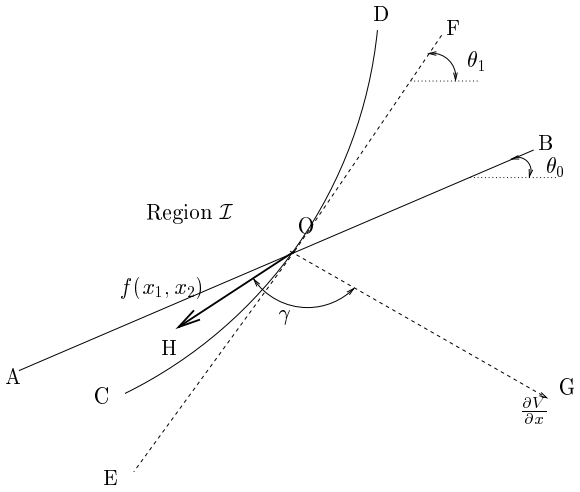

Figure 2.7: Intersection of a level curve with the line $\theta = \theta_0$.

$$\dot{x}(t_c) = \begin{bmatrix} \dot{x_1}(t_c) \\ x_2(t_c) \end{bmatrix} = f(x_1(t_c), x_2(t_c))$$

points out of the region $\mathcal{I}$.

Now refer to fig. 2.7. O denotes the point $(x_1(t_c), x_2(t_c))$. AOB is the line $\theta = \theta_0$ or $x_2 = \tan(\theta_0)x_1$ in Cartesian coordinates. COD is the level curve of V that passes through the point O. EOF is the tangent and OG is the outward normal to the level curve COD at the point O. Thus OG represents the vector $\partial V/\partial x$. OH is the vector $f(x_1, x_2)$ and as already explained it points out of region $\mathcal{I}$.

Let γ be the angle between the vectors $\vec{OH}$ and $\vec{OG}$. But since the vector $\vec{OG}$ points

away from the region $\mathcal{I}$ we have

$$\gamma \; < \; \pi/2 \; + \; \theta_1 \; - \; \theta_0 \tag{2.31}$$

and in light of Eqn. (2.23),

$$\gamma, \; [\pi/2 \; + \; \theta_1 - \theta_0] \; \in \; [0, \pi]. \tag{2.32}$$

Cosine is decreasing in the interval $[0, \pi]$, therefore

$$\cos\gamma \; > \; \cos[\pi/2 \; + \; \theta_1 \; - \; \theta_0]. \tag{2.33}$$

Note that

$$\cos\gamma \; = \; \left. \frac{(\frac{\partial V}{\partial x})^T \cdot f(x_1, x_2)}{\left\|\frac{\partial V}{\partial x}\right\| \, \|f(x_1, x_2)\|} \right|_{x_2 = x_1 \tan\theta_0} ; \tag{2.34}$$

this implies that

$$\left. \frac{(\frac{\partial V}{\partial x})^T . f(x_1, x_2)}{\left\|\frac{\partial V}{\partial x}\right\| \, \|f(x_1, x_2)\|} \right|_{x_2 = x_1 \tan\theta_0} \; > \; \cos[\pi/2 \; + \; \theta_1 - \theta_0] \tag{2.35}$$

which contradicts Eqn. (2.26). Hence all trajectories of the system in Eqn. (2.21) that originate in the region $\mathcal{Z}$ remain in the region $\mathcal{I}$ for all time. □

Similar lemmas may follow from considering cases other than $\theta_1 \geq \theta_0$ and for other forms of the invariant region $\mathcal{I}$; we will explore those cases as this research is ongoing. Now we present the main result of this chapter, a *rendezvous certificate theorem*.

Theorem 2.5.1 (Rendezvous certificate theorem)**.** Consider a system of two agents

$$\begin{aligned} \mathcal{V}_1 \; : \quad & \dot{x}_1 = f_1(x_1, x_2) \, ; \quad f_1(0,0) = 0, \\ \mathcal{V}_2 \; : \quad & \dot{x}_2 = f_2(x_1, x_2) \, ; \quad f_2(0,0) = 0, \end{aligned}$$

where x_1 and $x_2 \in \mathbb{R}$, and suppose that the origin is shown to be asymptotically stable under

a Lyapunov function of the form

$$V(x_1, x_2) = \frac{c_0({x_1}^2 + {x_2}^2)^{n/2}}{h\left(\tan^{-1}\left(\frac{x_2}{x_1}\right)\right)}$$

with positive real constants c_0 and $n \geq 1$, and with $h \in \mathcal{T}$. Consider a coverage angle θ_0 corresponding to a design specification ρ_{des} and identified with regions $\mathcal{I}$ and $\mathcal{Z}$. If a region $\mathcal{I}$ is an invariant region for the system, then the agents attain rendezvous in the region $\mathcal{R}$ around the origin within the design specification for all initial conditions lying in the region $\mathcal{Z}$.

Proof of Theorem 2.5.1: Follows from asymptotic stability of the origin and invariance of $\mathcal{I}$ with the associated Lyapunov function.

□

Note that the equation of any level set of the Lyapunov function V, eqn. (2.26) in polar coordinates is given by

$$r^n = \frac{\xi}{c_0} h(\theta).$$

This describes a many-one mapping from θ to r. In other words, for a given value of θ there are several values of real positive r. Thus invariance of $\mathcal{I}$, and hence rendezvous, can be examined unambiguously. In other words, since we know from Lemma 2.4.1, property 5, that all level sets cut the line $\theta = \theta_0$ with the same slope at the point of intersection, the right hand side of eqn. (2.26) is a constant.

Example 6. *Consider the following scenario from soccer: Suppose two members from one team are driving the soccer ball towards their opponent's goal. These two members are traveling along the edges of the field, with one member in possession of the ball. If the team member with the ball, identified as Player 1, is too close to the opponent goal keeper, the opponent goal keeper is capable of either intercepting Player 1 or intercepting a pass from Player 1 to Player 2. If a pass is made too early, the goal keeper is capable of intercepting Player 2 after a pass is made to him.*

Suppose these two players decide on the following strategy: Player 1 chooses to drive toward the goal, drawing the goal keeper toward him. In the meantime, Player 2 is also

running toward the goal. Just before the goal keeper can intercept Player 1, Player 1 makes a pass to Player 2. The pass must be made out of the reach of the goal keeper. Finally, before the goal keeper can intercept Player 2, Player 2 scores a goal. This is illustrated in the following figures.

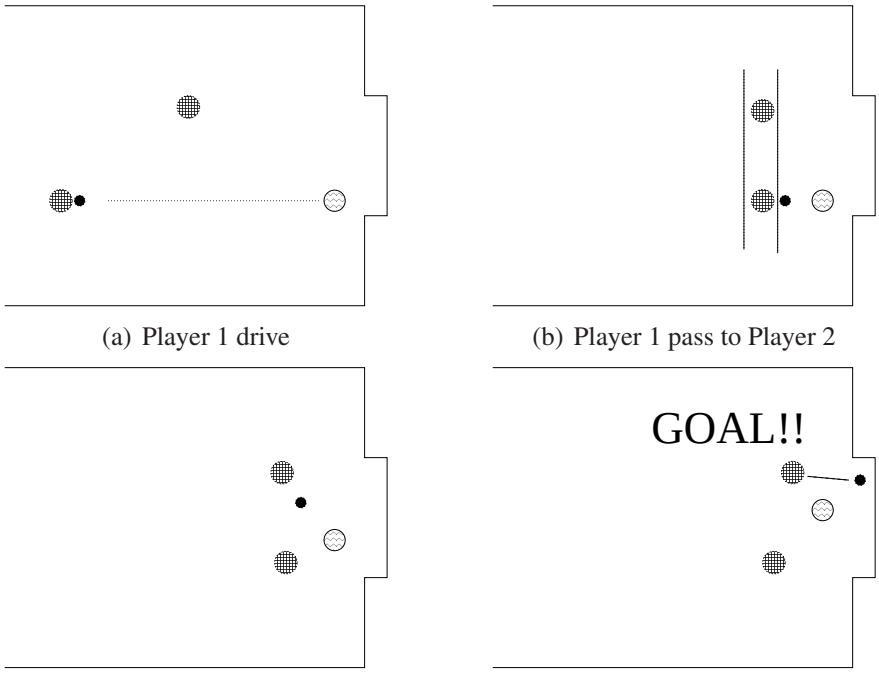

(a) Player 1 drive (b) Player 1 pass to Player 2

(c) Player 2 reception (d) Player 2 goal

Figure 2.8: Soccer strategy.

This scenario may be cast as a rendezvous problem. The trajectories of the two players are linear and so the dynamics of the two players may be represented by a system of two scalar agents. The combined events of the pass from Player 1 to Player 2 and the final attempt at the goal is representative of rendezvous. The constraint of avoiding (player or ball) interception by the goal keeper may be posed as a rendezvous performance problem. Suppose that the dynamics of the two players are represented by

$$\begin{aligned} \mathcal{V}_1 : \quad & \dot{x}_1 = -2x_1 - 4x_1(x_1^2 - x_2^2) \\ \mathcal{V}_2 : \quad & \dot{x}_2 = -2x_2 - 4x_2(x_2^2 - x_1^2), \end{aligned}$$

and suppose that the design specification given is $\rho_{des} = 2 - \sqrt{3}$. *Then with the Lyapunov*

function from eqn. (2.12) (repeated here for clarity),

$$V(x_1, x_2) = (x_1^2 + x_2^2)\left[a + be^{-8x_1^2x_2^2/d^2(x_1^2+x_2^2)^2}\right],$$

and according to the theorem, the agents attain rendezvous for any initial condition lying in the region $\mathcal{Z}$ as defined according to the specification. Note that the corresponding coverage angle is $\theta_0 = 15°$.

2.6 Concluding remarks

We have approached the rendezvous problem from the point of view of dynamics on the phase plane and of Lyapunov stability and invariance. On the phase plane, rendezvous can be realized in a rigorous fashion through the introduction of the rendezvous region $\mathcal{R}$ and coverage region $\mathcal{Z}$ with the respective design specifications δ and ρ_{des}. Because of this phase plane interpretation, Lyapunov stability theory can be directly applied to both the construction of controllers for rendezvous and the certification of achieving rendezvous. Lyapunov-function-based controller design is practical and intuitive for the rendezvous problem because achieving rendezvous bears a connection to achieving asymptotic stability, and because level sets of the control Lyapunov function are related to the system trajectories. A level set method was introduced for constructing Lyapunov functions for the purpose of rendezvous control. Trajectories that begin in certain invariant regions of phase space achieve rendezvous, which can be used to motivate Lyapunov function and controller design. Finally, a certificate theorem was given as a sufficient condition for rendezvous for a system, given the existence of invariant regions of phase space corresponding to a Lyapunov function that guarantees asymptotic stability of the rendezvous point.

The phase plane interpretation for the rendezvous problem has applications in many areas and this research is ongoing. For instance, it would be interesting to explore the notions of rendezvous region and coverage region for different geometries than those discussed here.

In addition, similar certificate theorems can be constructed for other families of Lya-

punov functions. The rendezvous problem may be recast to include systems of larger numbers of agents with general dynamics in the phase space of a higher dimension. We will study multi-agent rendezvous in the next chapter, I will also present a section on non-scalar agents. Necessary conditions could be explored for the rendezvous problem, and certificate theorems could be constructed for other types of rendezvous such as interception and avoidance.

Chapter 3

Cone invariance applied to rendezvous of multiple agents

3.1 Introduction

We defined the rendezvous problem in the previous chapter. In the rendezvous problem, one desires to have several agents arrive at predefined destination points simultaneously. As stated earlier, applications of the rendezvous problem include cooperative strike and jamming, ballistic missile interception, spacecraft docking, formation flying, and multi-agent consensus. The rendezvous control problem has been treated in [20], [22], and [23]. However, a systematic theory of multi-agent rendezvous is still to be explored.

In [20] and Chapter 2, we pose the two-scalar agent rendezvous problem as a combination of a cone invariance problem and a stability problem in a two-dimensional phase space. We presented a level set method of constructing control Lyapunov functions. Based on this method, we derived the main result of the chapter, a certificate theorem for guaranteeing approximate rendezvous. Using the ideas from Chapter 2, we pose the N-dimensional rendezvous problem on an N-dimensional phase space where the underlying closed-loop agent dynamics are linear. Because the underlying dynamics are linear, there exist quadratic control Lyapunov functions. Therefore, in this chapter we focus on satisfying cone invariance for multi-agent rendezvous.

Invariance of polyhedral domains is well studied in the literature([24], [25], [26]). Traditionally, polyhedral invariance has been used to study the linear constrained regulation

problem ([27], [28]) and problems with control and input saturation ([29]). Because of the nature of these problems, polyhedral invariance literature is well developed when the polyhedral set is represented in the constraint form (plane representation in [25]). However, in rendezvous applications, we employ a worst case analysis and thus we usually deal with polyhedral sets represented in the generator form (vertex representation in [25]). In this chapter, we derive invariance conditions for polyhedral cones represented in the generator form. Conical invariant sets have found applications in problems related to areas as diverse as industrial growth [30], ecological systems and symbiotic species [31], the arms race [32], and compartmental system analysis [33], [34]. Cone invariance is an essential component in problems involving competition or cooperation.

In Section 3.2 we introduce the notation used in the chapter and basic results from linear algebra. In Section 3.3 we represent the N scalar-agent rendezvous problem on the phase plane, and define constraints on the trajectories. In Section 3.4 we present a rendezvous certificate theorem. In Section 3.5 we analyze the implications of the cone invariance conditions on the eigen-structure of the closed-loop dynamics. In Section 3.6 we demonstrate the applicability of phase plane concepts to non-scalar agent rendezvous. In Section 3.7 we provide a summary of the results in this chapter and describe future research problems.

The results presented in this chapter have been published in [35].

3.2 Notations and mathematical preliminaries

In this section, I will introduce definitions and mathematical preliminaries needed for the results presented later in the chapter.

Definition 3.2.1. *A set S is said to be* positively invariant *with respect to the system $\dot{x} = f(x)$ if $x(0) \in S \implies x(t) \in S \ \forall t > 0$.*

Definition 3.2.2. *We will denote the 2^N hyper-octants of the vector space $\mathbb{R}^N$ as O_1, O_2, $\cdots$, O_{2^N}.*

Definition 3.2.3. *We denote the strict interior of a set $\mathcal{S}$ by int($\mathcal{S}$). The boundary of the set $\mathcal{S}$ will be denoted by ß($\mathcal{S}$).*

Lemma 3.2.1. *Let $v_1, v_2, \cdots, v_{2^N}$ be vectors in $\mathbb{R}^N$ such that $v_i \in int(O_i)$ then there exist $\alpha_i \in \mathbb{R}$, $\alpha_i \geq 0$ such that*

$$\alpha_1 v_1 + \alpha_2 v_2 + \cdots + \alpha_{2^N} v_{2^N} = 0 \tag{3.1}$$

Proof: If $v_i \in int(O_i)$, then origin lies in the interior of the convex hull of the vertices $v_1, v_2, \cdots, v_{2^N}$. □

Lemma 3.2.2. Let $v_1, v_2, \cdots, v_{2^N}$ be vectors in $\mathbb{R}^N$ such that

$$v_i \in int(O_i).$$

Then there is a set of N linearly independent vectors in the set of v_is. In other words, there exist indices $j_1, j_2, \cdots, j_N$ such that

$$v_{j_1}, v_{j_2}, \cdots, v_{j_N}$$

is a linearly independent set.

Proof: Let $e_i = [0, 0, \cdots, 1, 0, \cdots, 0]$ with 1 in the ith coordinate, then we shall show that $e_i \in span\{v_1, v_2, \cdots, v_{2^N}\}$. Renumber v_j's if necessary so that the ith coordinate of the first 2^{N-1} vectors is positive. Let u_j be the vector v_j without the ith coordinate. Then $u_1, \cdots, u_{2^{N-1}}$ are in different hyper-octants of $\mathbb{R}^{2^{N-1}}$. Therefore by Lemma 3.2.1 there exist nonnegative reals $\alpha_1, \cdots, \alpha_{2^{N-1}}$ such that

$$\alpha_1 u_1 + \alpha_2 u_2 + \cdots + \alpha_{2^{N-1}} u_{2^{N-1}} = 0$$

Hence

$$\alpha_1 v_1 + \alpha_2 v_2 + \cdots + \alpha_{2^{N-1}} v_{2^{N-1}} = \alpha e_i$$

with $\alpha > 0$. Hence $e_i \in span\{v_1, v_2, \cdots, v_{2^N}\}$. □

Definition 3.2.4. *The conical hull of the points $e_1, e_2, \cdots, e_m$ in $\mathbb{R}^N$ is the region defined by*

$$\{x \in \mathbb{R}^N : x = \alpha_1 e_1 + \alpha_2 e_2 + \cdots + \alpha_m e_m,\ \alpha_i \in \mathbb{R},\ \alpha_i \geq 0\}.$$

If $E \in \mathbb{R}^{N\times m}$ then the conical hull of the columns of E will be denoted as $Cone(E)$. The points $e_1, e_2, \cdots, e_m$ are called the generators for the cone $Cone(E)$.

Definition 3.2.5. *A polyhedral cone is the one that can be constructed by taking the conical hull of a finite number of generators.*

Definition 3.2.6. *A real $m \times m$ matrix T is said to be nonnegative if all its terms are non-negative, i.e.,*

$$T_{ij} \geq 0,\ \forall i, j.$$

I will denote this by

$$T \geq 0.$$

In order to distinguish from non-negative matrices, we use the following symbols to denote sign definiteness:

$$\begin{aligned}
T \text{ is symmetric positive definite} &\implies T \succ 0,\\
T \text{ is symmetric positive semidefinite} &\implies T \succeq 0,\\
T \text{ is symmetric negative definite} &\implies T \prec 0,\\
T \text{ is symmetric negative semidefinite} &\implies T. \preceq 0
\end{aligned}$$

Definition 3.2.7. *A real $m \times m$ matrix T is said to be essentially non-negative if all the off-diagonal terms are non-negative, i.e.,*

$$T_{ij} \geq 0,\ \forall i \neq j.$$

We will denote this by

$$T \overset{e}{\geq} 0.$$

Definition 3.2.8. *The spectral abscissa $r(A)$ of an $N\times N$ matrix A is defined as the maximum*

real parts of its eigenvalues.

$$r(A) = \max\{Re(\lambda) : \lambda \in spec(A)\}.$$

The following is a well known result in linear algebra and can be derived by extending Perron's results (Theorem 8.3.1 in [36]) for nonnegative matrices to essentially nonnegative matrices.

Lemma 3.2.3. If T is an $m \times m$ essentially non-negative matrix, then $r(T)$ is an eigenvalue of T and there is a non-negative vector $x \geq 0$, $x \neq 0$, such that $Tx = r(T)x$.

Proof: If $T \overset{e}{\geq} 0$ then there is some $\psi > 0$ such that $\psi I + T \geq 0$.

Note that x_i is an eigenvector of $\psi I + T$ with corresponding eigenvalue λ_i if and only if x_i an eigenvector of T with the corresponding eigenvalue $\lambda_i - \psi$. Now from Theorem 8.3.1 in [36] we know that the spectral radius $\rho(\psi I + T)$ is an eigenvalue of $\psi I + T$ with a nonnegative eigenvector. Hence $\rho(\psi I + T) - \psi$ is an eigenvalue of T with a nonnegative eigenvector. Now if λ_i are the set of eigenvalues of $\psi I + T$ then we have

$$Re(\rho(\psi I + T)) - \psi) \geq Re(\lambda_i - \psi)$$

Hence proved. □

3.3 N scalar-agent rendezvous

In this section we will define the rendezvous problem for N scalar agents trying to rendezvous at the origin of the real line. We consider N scalar agents with closed loop linear dynamics.

$$\dot{x} = Ax, \tag{3.2}$$

$$x = [x_1\ x_2\ \cdots\ x_N]^T, \quad x_i \in \mathbb{R}. \tag{3.3}$$

The development in this section is very similar to the cone invariance ideas developed

for the two scalar-agent case in Chapter 2.

Ideally, rendezvous for N scalar agents $\mathcal{V}_1$, $\mathcal{V}_2$, $\cdots$, $\mathcal{V}_N$ is said to be successful if all the N agents reach some neighborhood of the origin at precisely the same time as each other. To be consistent with Chapter 2 we will refer to this as the perfect rendezvous. For all practical purposes, it is sufficient that the agents reach this neighborhood within a short time interval of each other. We consider the following neighborhood around the origin (the rendezvous region):

$$\mathcal{R} = x \in \mathbb{R} : -\delta \leq x \leq \delta \text{ for some } \delta > 0. \tag{3.4}$$

We will represent this problem on the N-dimensional phase space. Define regions on the phase space

$$\begin{aligned} U_i &= \{(x_1, x_2, \cdots, x_N) \mid -\delta \leq x_i \leq \delta\}, \\ i &\in \{1, 2, \cdots, N\}. \end{aligned} \tag{3.5}$$

The arrival times of the agents in the rendezvous region $\mathcal{R}$ are

$$t_{\mathcal{V}_i} = \min\ [\ t \mid x(t) \in U_i\ ], \quad i \in \{1, 2, \cdots, n\}. \tag{3.6}$$

We define the earliest arrival time t_a as

$$t_a = \min(t_{\mathcal{V}_1}, t_{\mathcal{V}_2}, \cdots, t_{\mathcal{V}_N}). \tag{3.7}$$

The approximate rendezvous specification for the N scalar agents case can be written as

$$\rho = \frac{\max(|x_1(t_a)|, |x_2(t_a)|, \cdots, |x_N(t_a)|)}{\delta} \leq \rho_{\text{des}}. \tag{3.8}$$

For perfect rendezvous $\rho_{des} = 1$. Note that $\delta\rho_{\text{des}}$ is an upper bound on the infinity norm of the position of agents at the earliest time of arrival t_a. In other words, eqn. (3.8) means that

at the time of the earliest entry of an agent into the rendezvous region, the rest of the agents should not be farther than $\delta\rho_{des}$.

Consider the hyper-cube C of side $\delta(\rho_{des} - 1)$ in $\mathbb{R}^N$ whose body diagonal is the line joining the points

$$A = (\delta, \delta, \cdots, \delta)$$

and

$$B = (\delta\rho_{\text{des}}, \delta\rho_{\text{des}}, \cdots, \delta\rho_{\text{des}}).$$

Let Υ be the set of all the vertices of C except A and B. Define the polyhedral cone $\mathcal{I}$ as

$$\mathcal{I} = Cone(x : x \in \Upsilon).$$

Note that Υ has $2^N - 2$ points. I will call these points $e_1^\infty, e_2^\infty, \cdots, e_{2^N-2}^\infty$ as generators. The superscript ∞ is used to denote that these points are the boundary points under ∞ norm specification of approximate rendezvous. Define a matrix $\mathbb{R}^{N\times(2^N-2)}$ matrix E^∞ whose ith column is the coordinates of the point e_i^∞.

An important observation is that if the polyhedral cone $\mathcal{I}$ is positively invariant with respect to the system in eqn. (3.2) and if the system (3.2) is asymptotically stable then all trajectories of eqn. (3.2) that originate in the cone $\mathcal{I}$ satisfy the approximate rendezvous specification.

In the following example we demonstrate how to identify the cone $\mathcal{I}$ for $N = 3$.

Example 7. *Using the approximate rendezvous specification given in eqn. (3.8) for the three scalar agent case, the generator points e_1^∞ , e_2^∞ , $\cdots$, e_6^∞ in the positive orthant are*

found to be

$$\begin{aligned} e_1^{\infty} &= (\delta, \delta, \delta\rho_{des}) \\ e_2^{\infty} &= (\delta, \delta\rho_{des}, \delta) \\ e_3^{\infty} &= (\delta\rho_{des}, \delta, \delta) \\ e_4^{\infty} &= (\delta\rho_{des}, \delta\rho_{des}, \delta) \\ e_5^{\infty} &= (\delta\rho_{des}, \delta, \delta\rho_{des}) \\ e_6^{\infty} &= (\delta, \delta\rho_{des}, \delta\rho_{des}). \end{aligned}$$

The conical hull of the above points is the outer cone in fig. 3.1.

Note that the approximate rendezvous can also be specified in the 2 norm or 1 norm sense, our region $\mathcal{I}$ will be a second-order cone or a polyhedral cone with N generators, respectively.

The 2 norm case is dealt with in [37]. For the case of 1 norm the approximate rendezvous specification takes the form

$$|x_1(t_a)| + |x_2(t_a)| + \cdots + |x_N(t_a)| \leq \ \delta\rho_{\text{des}}. \tag{3.9}$$

For perfect rendezvous

$$\rho_{des} = N. \tag{3.10}$$

and for feasible approximate rendezvous

$$\rho_{des} \geq N \tag{3.11}$$

Eqn. (3.9) will give us N generator points in each of the hyper-octants. The invariant cones will be defined as the conical hull of the boundary points in each hyper-octant. In the following example we identify the desired invariant cone in $\mathbb{R}^3_+$.

Example 8. *Using the approximate rendezvous specification given in eqn. (3.9) for the three scalar agent case, the generator points* e_1^1 , e_2^1 *and* e_3^1 *in the positive orthant are found*

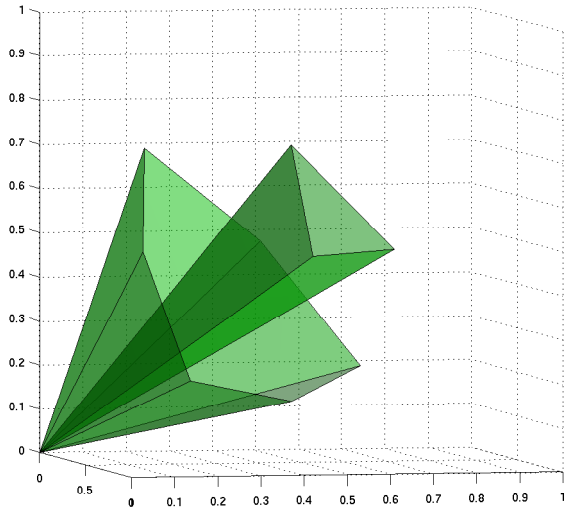

Figure 3.1: The desired invariant polyhedral cones under 1 norm and ∞ norm specifications for $\delta = 0.2$ and $\rho_{\text{des}} = 3.5$ in $\mathbb{R}^3_+$.

to be

$$\begin{aligned} e_1^1 &= (\delta, \delta, \delta(\rho_{des} - 2)) \\ e_2^1 &= (\delta, \delta(\rho_{des} - 2), \delta) \\ e_3^1 &= (\delta(\rho_{des} - 2), \delta, \delta). \end{aligned}$$

3.4 Rendezvous certificate

In this section, we first present a lemma on invariance of polyhedral cones. A similar result appears in [24]. Based on this lemma, we then state sufficient conditions for rendezvous of N scalar agents.

Lemma 3.4.1. Consider a system with closed-loop dynamics given by eqn. (3.2). Let e_1, $e_2, \cdots, e_m$ be points in $\mathbb{R}^N$ and let E be a matrix in $\mathbb{R}^{N \times m}$ constructed by choosing these points as columns. Then the region $Cone(E)$ is positively invariant with respect to system of eqn. (3.2) if and only if there exists an essentially non-negative $m \times m$ matrix T such that,

$$AE = ET. \tag{3.12}$$

Proof: (*Sufficiency*.) Assuming condition (3.12) holds, we need to prove the following implication:

$$x(0) \in Cone(E) \Rightarrow x(t) \in Cone(E),\ \forall t > 0. \tag{3.13}$$

Now, the equality in eqn. (3.12) implies that

$$A^k E = ET^k,\ \forall k \in \mathbb{N} \tag{3.14}$$

$$\Rightarrow\ e^{At}E = Ee^{Tt}. \tag{3.15}$$

Since $x(0) \in \mathcal{I}$, therefore there exists a non-negative vector $\alpha \in \mathbb{R}^m\ :\ \alpha \geq 0$, such that,

$$x(0) = E\alpha. \tag{3.16}$$

The expression for $x(t)$ is given as

$$x(t) = e^{At}x(0),\ \ \forall t \geq 0. \tag{3.17}$$

Substituting (3.16) in (3.17) and then using (3.15) we get

$$x(t) = Ee^{Tt}\alpha. \tag{3.18}$$

Now we will use the following classical result from [38]:
T essentially non-negative $\Leftrightarrow$ e^{Tt} non-negative: $e^{Tt} \geq 0, \forall t \geq 0$.

A non-negative square matrix multiplied by a non-negative vector will give me some non-negative vector β. Therefore,

$$x(t) = E\beta,\ \beta \geq 0. \tag{3.19}$$

Thus $x(t) \in Cone(E)$.
(*Necessity*.) To prove necessity we assume that implication (3.13) holds.

Let us represent $x(t)$ as

$$x(t) = E\alpha(t),\ \alpha(t) \geq 0\ \forall t \geq 0. \tag{3.20}$$

Now lets consider an infinitesimal move from the ith ray of the polyhedral cone. We consider a point x_i^0 on the ith ray given by

$$x_i^0 = E\alpha,\ \ \alpha_j = 0\ \forall j \neq i, \alpha_i = 1. \tag{3.21}$$

Differentiating (3.20) at x_i^0 gives us

$$\dot{x}(t)\Big|_{x=x_i^0} = E\dot{\alpha}(t)\Big|_{x=x_i^0} \tag{3.22}$$

$$\Rightarrow Ax_i^0 = E\dot{\alpha}(t)\Big|_{x=x_i^0} \tag{3.23}$$

$$\Rightarrow AE\begin{bmatrix} 0 \\ 0 \\ \vdots \\ 1 \\ \vdots \\ 0 \end{bmatrix} = E\dot{\alpha}(t)\Big|_{x=x_i^0}. \tag{3.24}$$

For a trajectory starting at $x = x_i^0$, to stay inside the polyhedral cone $\mathcal{I}$ I should have

$$\dot{\alpha}_j(t) \geq 0,\ \forall j \neq i. \tag{3.25}$$

Combining (3.24) and (3.25) we can rewrite

$$AE\begin{bmatrix}0\\0\\\vdots\\1\\\vdots\\0\end{bmatrix} = ET\begin{bmatrix}0\\0\\\vdots\\1\\\vdots\\0\end{bmatrix}, \tag{3.26}$$

where the ith column of the matrix T is given by

$$T_{ji} = \dot{\alpha}_j(t)\Big|_{x=x_i^0}. \tag{3.27}$$

Note that T is essentially non-negative by construction.

Similarly applying positive invariance for other rays of the polyhedral cone, we can prove that the action of AE is the same as the action of ET on a basis of $\mathbb{R}^m$.

Therefore, there exists a $\mathbb{R}^{m\times m}$ essentially non-negative matrix T such that $AE = ET$. □

The following is a certificate theorem for approximate rendezvous under ∞ norm specification:

Theorem 3.4.1. Consider N scalar agents with closed-loop dynamics

$$\dot{x} = Ax, \quad x \in \mathbb{R}^N.$$

If there exists a symmetric positive definite matrix $P \in \mathbb{R}^{N\times N}$ and an essentially non-negative matrix $T \in \mathbb{R}^{(2^N-2)\times(2^N-2)}$ such that

$$\left.\begin{aligned} AE^{\infty} &= E^{\infty}T \\ T &\overset{e}{\geq} 0 \end{aligned}\right\} \text{ Positive invariance and,}$$

$$\left.\begin{aligned} A^TP + PA &\prec 0 \\ P &\succ 0 \end{aligned}\right\} \text{ Asymptotic stability,}$$

where $E^{\infty} \in \mathbb{R}^{N \times 2^N - 2}$ is the matrix whose columns are the points $e_1^{\infty}, e_2^{\infty}, \cdots, e_{2^N-2}^{\infty}$, then the agents will achieve rendezvous with ∞ norm specification ρ_{des}, for all initial conditions lying in the region $Cone(E^{\infty})$.

Proof: The proof of Theorem 3.4.1 directly follows from Lemma 3.4.1 and a well known result on asymptotic stability of linear systems. □

Notes:

1. A similar result can be written down for the case when approximate rendezvous is specified in terms of 1 norm.

2. The conditions in the theorem are linear in T and P. Checking whether the conditions are satisfied is a convex feasibility problem.

Example 9. *Consider the closed-loop system of three scalar agents described by*

$$\dot{x} = \begin{bmatrix} -3.5 & 1.0607 & 1.0607 \\ 1.0607 & -4.25 & 0.75 \\ 1.0607 & 0.75 & -4.25 \end{bmatrix} x, \; x \in \mathbb{R}^3. \tag{3.28}$$

Suppose we want to attain rendezvous in the ∞ norm as well as the 1 norm sense for $\rho_{des} = 3.5$ and $\delta = 0.2$. The corresponding E matrices in the first quadrant are found to be:

$$E_1^{\infty} = \begin{bmatrix} 0.2 & 0.2 & 0.7 & 0.7 & 0.7 & 0.2 \\ 0.2 & 0.7 & 0.2 & 0.7 & 0.2 & 0.7 \\ 0.7 & 0.2 & 0.2 & 0.2 & 0.7 & 0.7 \end{bmatrix},$$

$$E_1^{1} = \begin{bmatrix} 0.2 & 0.2 & 0.3 \\ 0.2 & 0.3 & 0.2 \\ 0.3 & 0.2 & 0.2 \end{bmatrix}.$$

The eigenvalues of the closed-loop system are all negative so it is asymptotically stable. Feasible certificates were obtained for both the ∞ and 1 norm cases through solving the convex invariance conditions of Theorem 3.4.1.

Now consider the system

$$\dot{x} = \begin{bmatrix} -3.5 & 1.299 & 0.75 \\ 1.299 & -3.875 & 0.6495 \\ 0.75 & 0.6495 & -4.625 \end{bmatrix} x, \; x \in \mathbb{R}^3. \tag{3.29}$$

The eigenvalues of the closed-loop matrix have negative real parts as before. The invariance conditions also result in a feasible solution for the ∞ *norm case. However, for* 1 *norm the problem is infeasible.*

This example shows that for given values of ρ_{des} *and* δ, 1 *norm specifications impose stricter constraints on the trajectories than* ∞ *norm specifications. Fig. 3.2 shows some trajectories of the system in eqn.(3.29). Notice that while the trajectories are invariant with respect to the* ∞ *norm cone, they move in and out of the* 1 *norm cone.*

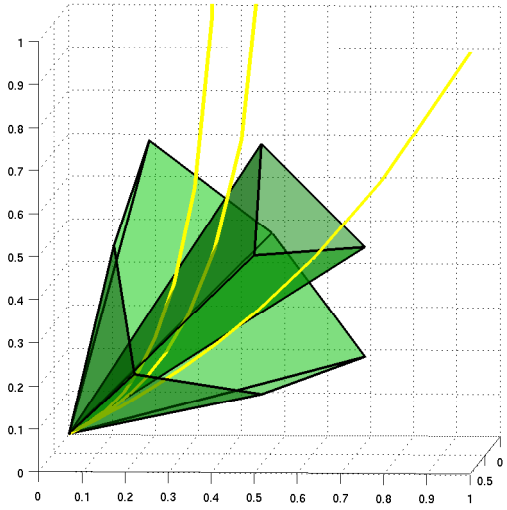

Figure 3.2: Trajectories invariant with respect to the outer cone but not the inner cone.

3.5 Implication of the invariance result on the eigen-structure of A

Theorem 3.4.1 only guarantees rendezvous for initial conditions lying in $Cone(E^{\infty})$, which lies completely inside the positive hyper-orthant. If rendezvous has to be guaranteed for initial conditions lying in all equivalent cones in all other hyper-orthants (for example the region $\mathcal{I}_1 \cup \mathcal{I}_2 \cup \mathcal{I}_3 \cup \mathcal{I}_4$ in fig. (3.3(a)) , then the required sufficient conditions are the collection of all invariance conditions for each of these cones. But as we will find out in this section, satisfying all such conditions imposes restrictions on the eigen-structure of the closed loop A matrix and results in solutions that are non-robust.

In this section we will present results for approximate rendezvous under both the ∞ norm and 1 norm specifications. Due to the non-singular nature of the E matrices in the case of 1 norm, the result is much stronger, as compared to the ∞ norm case. We first present results for the ∞ norm case.

Recall from Section 3.3, that for the ∞ norm case, the E^{∞} matrix in the positive hyper-orthant belongs to $\mathbb{R}^{N\times 2^N-2}$. If $\rho_{\text{des}} > 1$ then E^{∞} is full rank. From now on we will call the E^{∞} matrix in the positive hyper-orthant E_1^{∞}. The equivalent matrices in the other hyper-orthants will be numbered $E_2^{\infty}, E_3^{\infty}, \cdots, E_{2^N}^{\infty}$.

Note that $E_2^{\infty}, E_3^{\infty}, \cdots, E_{2^N}^{\infty}$ can be obtained from E_1^{∞} by multiplying it with a non-singular rotation matrix. Therefore $E_2^{\infty}, E_3^{\infty}, \cdots, E_{2^N}^{\infty}$ are also full rank. We will now state and prove the following lemma.

Theorem 3.5.1. Let $Cone(E_1^{\infty})$ be the desired invariant cone in the positive hyper-octant for ∞ norm approximate rendezvous specification $\rho_{\text{des}} > 1$ and let $Cone(E_2^{\infty})$, $Cone(E_3^{\infty})$, $\cdots$ and $Cone(E_{2^N}^{\infty})$ be the symmetric rotations of $Cone(E_1^{\infty})$ in the other hyper-octants. Now if all the above cones $Cone(E_1^{\infty})$, $Cone(E_2^{\infty})$, $\cdots$ and $Cone(E_{2^N}^{\infty})$ are positively invariant with respect to the system

$$\dot{x} = Ax, \quad x \in \mathbb{R}^N$$

then all eigenvalues of A are real.

Proof: $Cone(E_1^{\infty})$, $Cone(E_2^{\infty})$, $\cdots$ and $Cone(E_{2^N}^{\infty})$ are positively invariant with respect to

the above system; therefore, by Lemma 3.4.1 there exist essentially non-negative matrices $T_1, T_2, \cdots, T_{2^N}$, such that

$$\begin{aligned} AE_i^\infty &= E_i^\infty T_i, && (3.30)\\ T_i &\overset{e}{\geq} 0, && (3.31)\\ T_i &\in \mathbb{R}^{(2^N-2)\times(2^N-2)}. && (3.32) \end{aligned}$$

Now by Lemma 3.2.3, $r(T_i)$ is an eigenvalue of T_i and there exists $x_i \geq 0$, $x_i \neq 0$ such that

$$T_i x_i = r(T_i) x_i. \tag{3.33}$$

Multiplying both sides by E_i^∞ we get

$$\begin{aligned} E_i^\infty T_i x_i &= r(T_i) E_i^\infty x_i, && (3.34)\\ AE_i^\infty x_i &= r(T_i) E_i^\infty x_i. && (3.35) \end{aligned}$$

Now $E_i^\infty x_i \neq 0$ and $E_i^\infty x_i \in Cone(E_i^\infty)$; therefore, $r(T_i)$ is an eigenvalue of A and there exists a corresponding eigenvector in $Cone(E_i^\infty)$.

This means that A has 2^N eigenvectors in the strict interior of each orthant. Therefore by Lemma 3.2.2, N of these vectors are linearly independent. Therefore, all N eigenvalues of A are real and are given by the spectral abscissa of the T_i matrices. □

We are able to prove a stronger result under the 1 norm specification, which we present now:

Theorem 3.5.2. Let $Cone(E_1^1)$ be the desired invariant cone in the positive hyper-octant for 1 norm approximate rendezvous specification $\rho_{\text{des}} > N$ and let $Cone(E_2^1)$, $Cone(E_3^1)$, $\cdots$ and $Cone(E_{2^N}^1)$ be the symmetric rotations of $Cone(E_1^1)$ in the other hyper-octants. Now if all the above cones $Cone(E_1^1)$, $Cone(E_2^1)$, $\cdots$ and $Cone(E_{2^N}^1)$ are positively invariant with respect to the system

$$\dot{x} = Ax, \quad x \in \mathbb{R}^N$$

then A has a single real eigenvalue with algebraic multiplicity = geometric multiplicity =

N.

Proof: All steps of the proof for Theorem 3.5.1 hold by replacing the matrices E_i^∞ with the matrices E_i^1. In addition, now we know that $E_i^1 \in \mathbb{R}^{N\times N}$; therefore, the matrices A, T_1, $T_2, \cdots$ and T_{2^N} are similar. Thus we have

$$r(T_1) = r(T_2) = \cdots = r(T_{2^N}). \tag{3.36}$$

So all eigenvalues of A are the same with N linearly independent eigenvectors. □

Example 10 (Two scalar agent rendezvous)**.** *In this example we demonstrate Theorem 3.5.2 in the two dimensional phase space. In two dimensions the desired invariant cones are the same for both* ∞ *norm and* 1 *norm cases. The cone* $\mathcal{I}_1$ *in fig. 3.3(a) can be represented as*

$$\mathcal{I}_1 = Cone(E_1^1), \tag{3.37}$$

$$E_1^1 = \begin{bmatrix} \delta\rho_{des} & \delta \\ \delta & \delta\rho_{des} \end{bmatrix}. \tag{3.38}$$

The cones $\mathcal{I}_2$*,* $\mathcal{I}_3$*, and* $\mathcal{I}_4$ *can be generated by rotating* $\mathcal{I}_1$ *by* $\pi/2$*,* π*, and* $3\pi/2$ *radians, respectively, therefore,*

$$\mathcal{I}_i = Cone(E_i^1), \tag{3.39}$$

$$E_i^1 = R^{i-1}E_1^1, \quad i \in \{1,2,3,4\}, \text{ and} \tag{3.40}$$

$$R = \begin{bmatrix} 0 & -1 \\ 1 & 0 \end{bmatrix}. \tag{3.41}$$

Now from Lemma 3.5.2, if all the cones ($\mathcal{I}_1$*,* $\mathcal{I}_2$*,* $\mathcal{I}_3$*, and* $\mathcal{I}_4$*) are positively invariant w.r.t. the system*

$$\dot{x} = Ax, \quad x \in \mathbb{R}^2,$$

then A has a unique real eigenvalue with algebraic multiplicity = geometric multiplicity = 2. In other words the system $\dot{x} = Ax$ *has radial vector fields as shown in fig. (3.3(b)).*

Note:

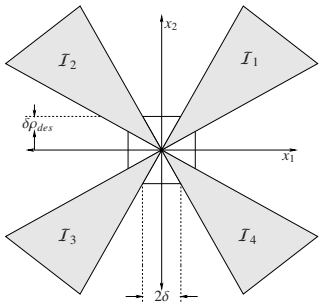

(a) The desired invariant cones for 2 scalar agent rendezvous

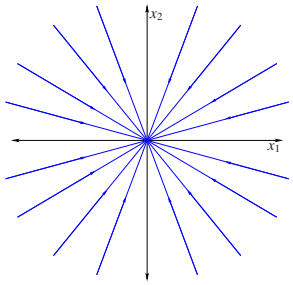

(b) Radial vector fields

Figure 3.3: Unique non-robust solution, if rendezvous is desired for trajectories originating in all quadrants.

- If $\rho_{\text{des}} > N$, the polyhedral cone corresponding to the 1 norm specification is fully contained in the corresponding polyhedral cone for the ∞ norm case. We conjecture that the only solution possible in the ∞ norm specification is the one that results in radial fields (all eigenvalues same and real).

- The radial fields solutions thus obtained are non-robust to disturbance and uncertainty. The trajectories live on the boundary of the polyhedral cone and can easily deviate out of the cone under uncertainty.

- If rendezvous is desired for initial conditions lying in all the hyper-octants, non-linear control design along the lines of [20] is likely to give a robust solution.

3.6 Non-scalar Agent Rendezvous

In this section we will demonstrate the applicability of the theory developed in Sections 3.3 and 3.4 to the case of non-scalar agents. We will demonstrate the simple case of two planar agents trying to rendezvous at the origin of $\mathbb{R}^2$.

Let us consider two planar vehicles with combined closed loop dynamics,

$$\begin{bmatrix} \dot{x}_1 \\ \dot{y}_1 \\ \dot{x}_2 \\ \dot{y}_2 \end{bmatrix} = A \begin{bmatrix} x_1 \\ y_1 \\ x_2 \\ y_2 \end{bmatrix}, \tag{3.42}$$

where $x_i, y_i \in \mathbb{R}$.

In fig. 3.4(a), the rendezvous task for agents 1 and 2 is to reach the inner square of side δ around origin within a small time interval of each other. To accomplish this task, we require that at the first instant when one agent enters the inner square, the other agent should be at least inside the outer square of side $\delta\rho_{\text{des}}$. To state this condition formally we define

$$\begin{aligned} t_{\mathcal{V}_i} &= \min \left[t \ : \ \max\{|x_i(t)|, |y_i(t)|\} \leq \delta \right], \\ i &\in \{1, 2\}, \\ t_a &= \min \{t_{\mathcal{V}_1}, t_{\mathcal{V}_2}\}. \end{aligned}$$

In this sense, $t_{\mathcal{V}_i}$ is the arrival time of the ith agent to the inner square; therefore for successful rendezvous,

$$\max_i \left[\max\{|x_i(t_a)|, |y_i(t_a)|\}\right] \leq \delta\rho_{\text{des}}. \tag{3.43}$$

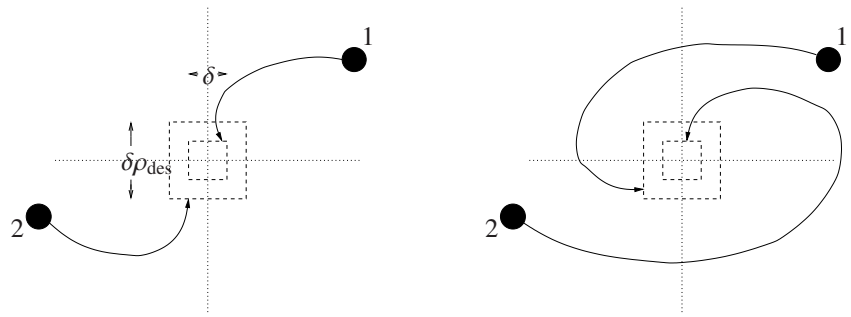

(a) Planar rendezvous (b) Limitations of Theorem 3.6.1.

Figure 3.4: Planar rendezvous condition is sufficient but not necessary

Define the region $\mathcal{W} \in \mathbb{R}^4$ as

$$\mathcal{W} = \left(\left[\begin{array}{c} x_1 \\ y_1 \\ x_2 \\ y_2 \end{array} \right] : \begin{array}{ccccc} \frac{1}{\rho_{\text{des}}} & \leq & \left|\frac{x_1}{x_2}\right| & \leq & \rho_{\text{des}} \\ \\ \frac{1}{\rho_{\text{des}}} & \leq & \left|\frac{y_1}{y_2}\right| & \leq & \rho_{\text{des}} \end{array} \right). \tag{3.44}$$

In order to guarantee rendezvous for all initial conditions lying in $\mathcal{W}$, we will break down the planar rendezvous problem into two scalar rendezvous problems. The idea is, that if x_1, x_2 and y_1, y_2 attain rendezvous in their respective two-dimensional phase spaces, then rendezvous will be successful on the plane.

We define the matrix E_1^{planar} as

$$E_1^{\text{planar}} = \left[\begin{array}{cccc} \delta & \rho_{\text{des}} & 0 & 0 \\ 0 & 0 & \delta & \rho_{\text{des}} \\ \rho_{\text{des}} & \delta & 0 & 0 \\ 0 & 0 & \rho_{\text{des}} & \delta \end{array} \right]. \tag{3.45}$$

It is easy to verify the following result:

Lemma 3.6.1.

$$\left[\begin{array}{cccc} x_1 & y_1 & x_2 & y_2 \end{array} \right]^T \in Cone(E_1^{\text{planar}}) \tag{3.46}$$

if and only if

$$\left[\begin{array}{c} x_1 \\ x_2 \end{array} \right] \in Cone\left(\left[\begin{array}{cc} \delta & \delta\rho_{\text{des}} \\ \delta\rho_{\text{des}} & \delta \end{array} \right] \right), \tag{3.47}$$

$$\left[\begin{array}{c} y_1 \\ y_2 \end{array} \right] \in Cone\left(\left[\begin{array}{cc} \delta & \delta\rho_{\text{des}} \\ \delta\rho_{\text{des}} & \delta \end{array} \right] \right). \tag{3.48}$$

Now we can state the rendezvous certificate theorem for planar rendezvous,

Theorem 3.6.1. If the system in eqn.(3.42) is asymptotically stable and there exists a 4×4

matrix T such that

$$AE_1^{\text{planar}} = E_1^{\text{planar}} T, \tag{3.49}$$

$$T \overset{e}{\geq} 0, \tag{3.50}$$

then one can guarantee rendezvous for all initial conditions such that

$$\begin{aligned} x_i(0), y_i(0) &\geq 0 \\ \begin{bmatrix} x_1(0) & y_1(0) & x_2(0) & y_2(0) \end{bmatrix}^T &\in \mathcal{W}. \end{aligned}$$

Proof: The proof follows from Lemmas 3.4.1 and 3.6.1. □

It is important to note that this theorem only provides sufficient conditions for rendezvous and yields certificates for trajectories where an agent never crosses from one quadrant to another on the plane. For instance, although the trajectories shown in fig. 3.4(b) achieve successful planar rendezvous, the trajectories violate the invariance conditions required by the theorem. Deriving a more general certificate theorem that covers these cases is an avenue of future research.

3.7 Conclusions and Future work

In this chapter, I have extended the concepts outlined in Chapter 2 to the case of N scalar agents and have demonstrated their utility for non-scalar agents. While in Chapter 2 we considered two scalar agents with non-linear dynamics, in this chapter the underlying dynamics are always assumed to be linear. I have employed the theory of invariance of polyhedral regions to derive a set of convex conditions, which when feasible yield a certificate of successful rendezvous. I have also shown that if rendezvous certificates are desired for initial conditions lying in a much larger symmetric set around the origin, the problem is over-constrained. The only feasible closed-loop linear dynamics that satisfy this over-constrained problem are the ones with radially decaying vector fields. All such solutions are non-robust to uncertainties. This suggests that for robustness in the over-constrained

case, we need to use non-linear synthesis.

The problem of designing a linear state feedback controller for rendezvous of N scalar agents can form a good future extension of this work. A first attempt at the synthesis problem led me to a set of conditions that are bilinear. There is some literature ([39], [40]) on a method to minimize the spectral abscissa of an essentially non-negative matrix under cone invariance constraints. In our work on rendezvous using second order cones [41], we present a detailed solution of the rendezvous synthesis problem. Future directions also include introducing uncertainty and communication link failure between the cooperating agents.

Chapter 4

Stochastic algorithms for dynamic sensor coverage

4.1 Introduction

Sensor coverage is the problem of deploying multiple sensors in an unknown environment for the purpose of automatic surveillance, cooperative exploration, or target detection. Recent years have witnessed increased interest among the communication, control, and robotics researchers in the area of mobile sensor networks. Each individual node in such a network has sensing, computation, communication, and locomotion capabilities. When the environment is rapidly changing, finding an efficient deployment strategy becomes a key issue for any application.

Coverage can be static (fixed sensors) or dynamic (mobile sensors). Static sensor coverage is desirable if the area to be covered is less than the union of the ranges of the sensor nodes. Static sensor coverage problem has been considered in [42] and in the references therein. The dynamic sensor coverage becomes necessary when a limited number of sensors is available and the area of interest cannot be covered by a static configuration of sensors. There have been attempts to empirically solve the dynamic coverage problem using simulations and actual robots [43] but a sound theoretical base is still missing in the literature.

In this chapter I consider N discrete time linear systems located at different points in space. One may think of dividing the uncertain area under consideration using a grid and

then these N systems can be thought to represent the dynamics of local environment change at the grid points. I analyze the case when a single sensor is deployed. The sensor maintains discrete time Kalman filter estimates of the states of all the N systems. In order to model the limited range of the sensor, I constrain the sensor to receive measurements only for the system where it is physically located at that time instant. All the tools developed in this chapter can be applied to the case where multiple grid points fall in the sensory range and hence the sensor receives measurements from more than one system. This extension requires only minor modifications and is left as a future research direction.

For a system where the sensor is located, the sensor implements both the time update and measurement update laws of the Kalman filter. For all the other systems for which the sensor did not receive any measurements, only the time update law is implemented. The motion of the sensor is an i.i.d. random process under the first strategy and a discrete time discrete state (DTDS) Markov chain in the later strategy. For successful coverage the sensor needs to hop from one system to another such that the error covariance matrices of the estimates of states of all N systems are bounded at all times. Intuition tells us that the sensor should spend more time at a location where the environment is changing rapidly than at one where the dynamics are relatively slow. The results I present in this chapter satisfy this intuition. A similar set of results, developed independently, have been presented in [44]

In Section 4.2 I describe the problem mathematically. In Section 4.3 and 4.4 I present success and failure results for a single sensor moving according to two different motion strategies. In Section 4.5, I conclude and identify future research directions.

The results presented in this chapter have been published in [45].

4.2 Problem Description

Consider N independently evolving LTI systems, whose dynamics are given by

$$\begin{cases} x_{i,k+1} = A_i x_{i,k} + w_{i,k} \\ y_{i,k} = C_i x_{i,k} + v_{i,k} \end{cases}, \tag{4.1}$$

where $x_{i,k},\ x_{i,k+1},\ w_{i,k} \in \mathbb{R}^{n_i}$ and $y_{i,k},\ v_{i,k} \in \mathbb{R}^{m_i}$, w_i and v_i are Gaussian random vectors with zero mean and covariance matrices Q_i and R_i, respectively, and i takes values in the set $\{1, 2, 3, \cdots, N\}$. Let $\mathbb{S}_n(\mathbb{S}_n^+)$ denote the set of symmetric positive semidefinite(definite) matrices of dimension n.

As already mentioned, the space to be covered can be discretized using a grid, and the above N systems can be thought to represent the dynamics of certain local variables at the grid points. These variables can be temperature, barometric pressure in case of weather monitoring, threat emergence rate in case of surveillance, uncertain location of adversaries and friends in a situational awareness task, and congestion measures at various routers in the case of a network.

In reality the independent evolution of the systems assumption may not always hold, as the dynamics of systems proximate in space may be highly dependent or even coupled. The results for the coupled environment case are under development, but the basic intuition and insight into the coverage problem remain the same.

There are N possible locations at which the sensor can be at a given time. If the sensor is in state i at time k it only has access to the measurement of the ith system at that time. The state transitions occur at a fixed time interval, which is assumed to be the same as the sampling period of all the N systems without any loss of generality.

The sensor runs N Kalman filter recursions, one for each of the N systems. For system i the time update equations of the Kalman filter are implemented at all time instants, whereas the measurement update equations are implemented only at those time instants when the sensor happens to be at location i.

Let S_k be the stochastic process describing the motion of the sensor. S_k takes values in the set $\{1, 2, 3, \cdots, N\}$. Let $I_{i,k}$ be the indicator function describing whether or not the sensor is at location i at time k. Therefore $I_{i,k} = 1$ if and only if $S_k = i$. We model the covariance matrix of the measurement noise for the ith system in the following manner:

$$Var(v_{i,k}) = \begin{cases} R_i, & I_{i,k} = 1 \\ {\sigma_i}^2 I, & I_{i,k} = 0 \end{cases}.$$

When the sensor is not at location i no observation is made for system i and this corresponds to the limiting case of $\sigma \to \infty$. Following a similar approach as in [46] we get the following Kalman filter equations:

$$\hat{x}^-_{i,k+1} = A_i \hat{x}_{i,k}, \tag{4.2}$$

$$P^-_{i,k+1} = A_i P_{i,k} A_i^T + Q_i, \tag{4.3}$$

$$\hat{x}_{i,k+1} = \hat{x}^-_{i,k+1} + I_{i,k+1} P^-_{i,k+1} C_i^T (C_i P^-_{i,k+1} C_i^T + R_i)^{-1} (y_{i,k+1} - C_i \hat{x}^-_{i,k+1}), \tag{4.4}$$

$$P_{i,k+1} = P^-_{i,k+1} - I_{i,k+1} P^-_{i,k+1} C_i^T (C_i P^-_{i,k+1} C_i^T + R_i)^{-1} C_i P^-_{i,k+1}. \tag{4.5}$$

Eqn. (4.2) and eqn. (4.3) are the time update relations for the estimate and the error covariance. It can be clearly seen from eqn. (4.4) and eqn. (4.5) that the measurement update is performed only when the sensor is at location i.

Using the above equations the recursive relation for the *a priori* error covariance matrix can be written as

$$P^-_{i,k+1} = A_i P^-_{i,k} A_i^T + Q_i - I_{i,k+1} A_i P^-_{i,k} C_i^T (C_i P^-_{i,k} C_i^T + R_i)^{-1} C_i P^-_{i,k} A_i^T. \tag{4.6}$$

For the rest of the chapter I will drop the $-$ superscript from $P^-_{i,k}$. An important observation is that eqn. (4.6) is stochastic in nature due to presence of the random variable $I_{i,k+1}$. We now have N of these stochastic recursive equations, one for each of the N systems. So to maintain an appreciable estimate of the states of all N systems we would want that the $\lim_{k\to\infty} \mathbb{E}[P_{i,k}]$ remain bounded for all i.

Since both $I_{i,k+1}$ and $P_{i,k}$ are random variables, we know that

$$\mathbb{E}[P_{i,k+1}] = \mathbb{E}[\mathbb{E}[P_{i,k+1}|P_{i,k}]], \tag{4.7}$$

where the inner expectation operator is over $I_{i,k+1}$ and the outer expectation is over $P_{i,k}$. Therefore,

$$\mathbb{E}[P_{i,k+1}] = \mathbb{E}[A_i P_{i,k} A_i^T + Q_i - \rho_{i,k+1} A_i P_{i,k} C_i^T (C_i P_{i,k} C_i^T + R_i)^{-1} C_i P_{i,k} A_i^T], \tag{4.8}$$

where $\eta_{i,k+1} = \Pr[I_{i,k+1} = 1|P_{i,k}]$.

Definition 4.2.1. *The dynamic sensor coverage problem is considered successfully solved if the N limits*

$$\lim_{k\to\infty} \mathbb{E}[P_{i,k}]\ ,\ i \in \{1, 2, \cdots, N\}$$

are finite for any set of initial conditions $P_{i,0} \geq 0$.

If there exists an $i \in \{1, 2, \cdots, N\}$ *such that* $\lim_{k\to\infty} \mathbb{E}[P_{i,k}]$ *is unbounded for some* $P_{i,0} \geq 0$*, then the sensors have failed to solve the dynamic coverage problem.*

Based on the above definition, we now present success and failure results for two different sensor motion strategies for a single sensor.

4.3 S_k independent and identically distributed

Under this strategy, at each time instant the sensor chooses to visit location i with probability π_i, which is independent of the history of S_k. In this case $\eta_{i,k+1} = \Pr[I_{i,k+1} = 1|P_{i,k}]$ $= \Pr[I_{i,k+1}] = \pi_i$. So (4.8) reduces to

$$\mathbb{E}[P_{i,k+1}] = \mathbb{E}[A_i P_{i,k} A_i^T + Q_i - \pi_i A_i P_{i,k} C_i^T (C_i P_{i,k} C_i^T + R_i)^{-1} C_i P_{i,k} A_i^T]. \tag{4.9}$$

Now this equation is exactly the same as the one analyzed in [46] for packet-based networks. The following two results easily follow.

Proposition 4.3.1. *Consider the system in eqn. (4.1). Let* $(A_i, \sqrt{Q_i})$ *be controllable,* (A_i, C_i) *be detectable, and* A_i *be unstable for all i. The sensor motion is governed by an i.i.d. distribution with Prob*$[S_k = i] = \pi_i$*. Now if*

$$\sum_{i=1}^{N} \frac{1}{\alpha_i^2} < N - 1, \tag{4.10}$$

where α_i *is the spectral radius of* A_i*, then a single sensor fails to solve the dynamic coverage problem.*

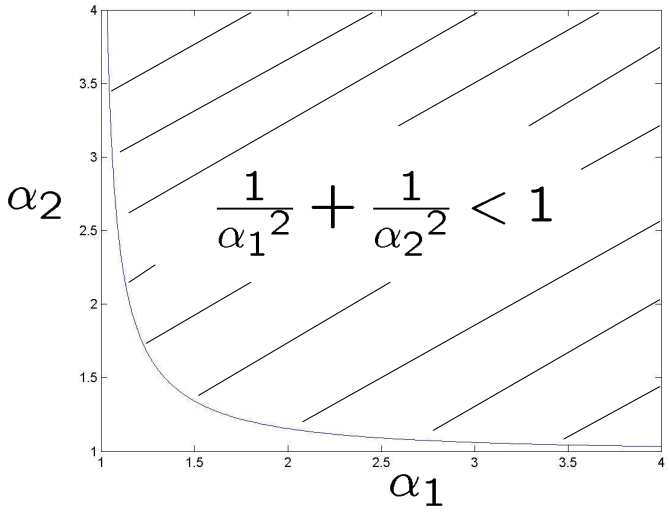

Figure 4.1: Failure region

Proof:

$$\sum_{i=1}^{N} \frac{1}{\alpha_i^2} < N - 1 \Longrightarrow \sum_{i=1}^{N} \left(1 - \frac{1}{\alpha_i^2}\right) > 1.$$

Therefore for any steady state probability vector π there exists an i s.t. $\pi_i < 1 - 1/{\alpha_i}^2$. Now from [46] we know that $\lim_{k\to\infty} \mathbb{E}[P_{i,k}]$ is unbounded for some initial condition $P_{i,0} \geq 0$. Thus a single sensor cannot solve the dynamic sensor coverage problem. □.

It can be seen that eqn. (4.10) is a measure of how fast the systems evolve. In Fig. 4.1 the region above the curve is where a single sensor fails to solve the dynamic coverage problem for two systems. It should be noted that if one system is evolving very slowly then the sensor can tolerate very fast dynamics of the other system before it fails. In such a scenario the sensor distributes its time, spending relatively large amount of time observing the fast system.

I now give some conditions under which it's possible to solve the dynamic sensor coverage problem by employing a single sensor. Before that I need to carry over a few terms from [46].

For real symmetric Y, define $\Psi_i(Y,Z)$ as

$$\Psi_i(Y,Z) = \begin{bmatrix} Y & \sqrt{\pi}(YA_i + ZC_i) & \sqrt{1-\pi}YA_i \\ \sqrt{\pi}(A_i'Y + C_i'Z') & Y & 0 \\ \sqrt{1-\pi}A_i'Y & 0 & Y \end{bmatrix}$$

and π_i^u as

$$\pi_i^u = \arg\min_{\pi} (\exists 0 \leq Y \leq I, Z \mid \Psi_i(Y,Z) > 0).$$

Proposition 4.3.2. *Let sensor motion be an i.i.d. process with distribution π. If $\sum_{i=1}^N \pi_i^u < 1$ and if π lies in the convex hull of the N points, a_i, $i = 1, \cdots, N$, defined as*

$$a_i = \begin{bmatrix} \pi_1^u & \cdots & \pi_{i-1}^u & 1-\sum_{k\neq i}\pi_k^u & \pi_{i+1}^u & \cdots & \pi_N^u \end{bmatrix}^T,$$

then the dynamic coverage problem is solved.

Proof: Since π lies in the convex hull of the above points, therefore there exist $\beta_i \geq 0$, $\sum_i \beta_i = 1$, s.t.

$$\begin{aligned} \pi_j &= \pi_j^u \sum_{i\neq j}\beta_i + \beta_j(1 - \sum_{i\neq j}\pi_i^u) \\ &= \pi_j^u(1-\beta_j) + \beta_j(1 - \sum_{i\neq j}\pi_i^u) \\ &> \pi_j^u(1-\beta_j) + \beta_j\pi_j^u \\ &= \pi_j^u. \end{aligned}$$

Now, it was shown in [46] that if $\pi_i > \pi_i^u$ then $\mathbb{E}[P_{i,k}]$ remains bounded as $k \to \infty$ for all initial conditions $P_{i,0} \in \mathbb{S}_{n_i}$, and hence the result follows. □

4.4 S_k varies according to an ergodic Markov process

In this section we will let S_k be a discrete time discrete state DTDS Markov process with transition probability matrix $\mathcal{T}$. $\mathcal{T}_{ij}$ is the probability that the sensor will be at location j at time $k+1$ given that it is in location i at time k. If $\pi_{i,k}$ is the probability of finding the

sensor in location i at time k, then the column vector π_k follows the recursion

$$\pi_{k+1}^T = \pi_k^T \mathcal{T}.$$

This kind of model is better for sensor motion because there may be physical constraints on the motion of the sensor. For example, the sensor may not be able to move between two systems located far away in space in one time interval. Such restrictions can be imposed by making the corresponding transition probability between such states equal to zero.

Markov chains have been used earlier for search and surveillance problems in the operations research community [47].

Under the ergodicity assumption we know that the Markov chain S_k has a unique steady state distribution and $\lim_{k\to\infty} \pi_k = \pi$ for all initial probability distributions. [**?**]

For the analysis of the Markov chain case we define the following relations for $X \in \mathbb{S}_n$.

$$h(X) \triangleq AXA' + Q, \tag{4.11}$$

$$f(X) \triangleq AXC'(CXC' + R)^{-1}CXA', \tag{4.12}$$

$$g(X) \triangleq h(X) - f(X). \tag{4.13}$$

In the rest of this chapter $h_i(X)$, $g_i(X)$, and $f_i(X)$ will refer to the same functional forms as described above but with parameters of system i. For example, $h_i(X) = A_i X A_i' + Q_i$ for $i \in \{1, 2, \cdots, N\}$. At this point we would like to remind the reader that under the estimation scheme described in Section 2. the recursion of the error covariance matrix of location i can be written in terms of h_i and g_i as

$$P_{i,k+1} = \begin{cases} h_i(P_{i,k}) & S_k \neq i \\ g_i(P_{i,k}) & S_k = i \end{cases}. \tag{4.14}$$

We now present some preliminary results required to prove our main theorem.

Lemma 4.4.1. *If $X \geq Y$, then $g(X) \geq g(Y)$ and $h(X) \geq h(Y)$.*

Proof: See [46]. □

Lemma 4.4.2. *If $U \in \mathbb{S}_n^+$ and $V \in \mathbb{S}_n$, then $\exists$ a scalar $t \geq 0$ such that $tU - V \in \mathbb{S}_n$.*

Proof: By Weyl's Theorem [48], $t \geq 0$

$$\begin{aligned} \lambda_{min}(tU - V) &\geq \lambda_{min}(tU) + \lambda_{min}(-V), \\ &= t\lambda_{min}(U) - \lambda_{max}(V), \end{aligned}$$

where λ_{min} is the minimum eigenvalue and λ_{max} is the maximum eigenvalue. So any $t \geq \frac{\lambda_{max}(V)}{\lambda_{min}(U)}$ proves the lemma. Such a t always exists because $\lambda_{min}(U) > 0$. □

Lemma 4.4.3. *$g(X) \geq Q, \forall X \geq 0$ and if C is invertible then, $g(X) \leq AC^{-1}RC^{'-1}A' + Q, \forall X \geq 0$.*

Proof: Clearly $g(X) \geq g(0) = Q$. For any $X \geq 0$, as $C^{-1}RC^{'-1} \in \mathbb{S}_n^+$, by Lemma 4.4.2, $\exists t \geq 0$ such that

$$\begin{aligned} X &\leq tC^{-1}RC^{'-1}, \\ g(X) &\overset{a}{\leq} g(tC^{-1}RC^{'-1}), \\ &= t/(t+1)AC^{-1}RC^{'-1}A' + Q, \\ &\leq AC^{-1}RC^{'-1}A' + Q, \end{aligned}$$

by using Lemma 4.4.1 in a. □

Lemma 4.4.4. *(a) If A is unstable then*

$$\lim_{k\to\infty} h^k(X_0) = \infty, \ \forall X_0 \in \mathbb{S}_n.$$

(b) If the spectral radius of A, $\alpha < 1$ and the pair $(A, \sqrt{Q})$ is observable, then the Lyapunov difference equation $X_{k+1} = h(X_k)$ converges to a unique positive semi-definite solution $T > 0$ as $k \to \infty$. In other words the following infinite sum

$$\lim_{k\to\infty} \left[A^k X_0 A'^k + \sum_{m=0}^{k-1} A^m Q A'^m \right]$$

is a finite positive definite matrix $T > 0$ for all $X_0 \geq 0$, where $T = h(T)$.

Proof: See [49]. □

The following probabilities will be useful in our analysis. The derivation is relatively simple and we omit the proofs due to space constraints. $\mathcal{T}_{ii}$ is the ith diagonal entry of the transition probability matrix and π_i is the steady state probability of finding the sensor at location i.

$$\begin{aligned}
\rho_{i,hh} = \Pr[S_{k+1} \neq i | S_k \neq i] &= \frac{1 - \pi_i(2 - \mathcal{T}_{ii})}{1 - \pi_i}, \\
\rho_{i,hg} = \Pr[S_{k+1} = i | S_k \neq i] &= 1 - \rho_{i,hh}, \\
\rho_{i,gg} = \Pr[S_{k+1} = i | S_k = i] &= \mathcal{T}_{ii}, \\
\rho_{i,gh} = \Pr[S_{k+1} \neq i | S_k = i] &= 1 - \rho_{i,gg}.
\end{aligned} \tag{4.15}$$

Theorem 4.4.1. *(a) Let (A_i, C_i) be detectable and $(A_i, \sqrt{Q_i})$ be observable, and if the sensor motion is described by an ergodic Markov chain S_k then the sensor fails to solve the dynamic coverage problem if at least one of the following conditions holds:*

$$\rho_{i,hh} = \frac{1 - \pi_i(2 - \mathcal{T}_{ii})}{1 - \pi_i} > \frac{1}{{\alpha_i}^2}, i \in 1, 2 \cdots N,$$

where α_i is the spectral of A_i.

(b) If in addition all C_is are invertible then the sensor solves the Dynamic Coverage problem, if all the following conditions hold:

$$\rho_{i,hh} = \frac{1 - \pi_i(2 - \mathcal{T}_{ii})}{1 - \pi_i} < \frac{1}{{\alpha_i}^2}, i \in 1, 2 \cdots N.$$

Proof: For simplicity we prove this result for the case when the initial probability distribution of the sensor is the same as the steady state distribution. In practice if one knows the transition probability matrix of a Markov chain, implementing such a constraint is easy.

Table 4.1: Illustration of how to find the lower bound.

Probabilities	Values	Lower bounds
$(1-\pi_i)\rho_{i,hh}^2$	$h_i^3(P_{i,0})$	$h_i^3(P_{i,0})$
$\pi_i\rho_{i,gh}\rho_{i,hh}$	$h_i^2 g_i(P_{i,0})$	$h_i^2(Q_i)$
$(1-\pi_i)\rho_{i,hg}\rho_{i,gh}$	$h_i g_i h_i(P_{i,0})$	$h_i(Q_i)$
$\pi_i\rho_{i,gg}\rho_{i,gh}$	$h_i g_i^2(P_{i,0})$	$h_i(Q_i)$
$(1-\pi_i)\rho_{i,hh}\rho_{i,hg}$	$g_i h_i^2(P_{i,0})$	Q_i
$\pi_i\rho_{i,gh}\rho_{i,hg}$	$g_i h_i g_i(P_{i,0})$	Q_i
$(1-\pi_i)\rho_{i,hg}\rho_{i,gg}$	$g_i^2 h_i(P_{i,0})$	Q_i
$\pi_i\rho_{i,gg}^2$	$g_i^3(P_{i,0})$	Q_i

(a) $P_{i,k+1}$ can take 2^{k+1} different values with different probabilities for a given value of $P_{i,0}$ depending on the values of $S_1, S_2 \cdots S_{k+1}$. From Lemma 4.4.3 we know that $g_i(X) \geq Q_i$, and from Lemma 4.4.1 we know that h_i is an increasing function. Therefore,

$$\mathbb{E}[P_{i,k}] \geq \pi_i Q_i + \frac{(1-\pi_i)}{\rho_{i,hh}}\rho_{i,hh}^k h_i^k(P_{i,0}) + \frac{\pi_i\rho_{i,gh}}{\rho_{i,hh}}\sum_{m=0}^{k-2}\rho_{i,hh}^{m+1}h_i^{m+1}(Q_i) \tag{4.16}$$

To illustrate how we obtain the above inequality we consider the case when $k = 3$, in table 4.4. The right hand side of the above equation is the inner product of the first and third rows of the table. Using Lemma 4.4.4 the sensor would fail to solve the dynamic coverage problem if the following condition holds for at least one system i.

$$\rho_{i,hh} = \frac{1-\pi_i(2-\mathcal{T}_{ii})}{1-\pi_i} > \frac{1}{{\alpha_i}^2}.$$

(b) If C_is are invertible then we can find an upper bound using Lemma 4.4.3

$$\mathbb{E}[P_{i,k}] \leq \pi_i M_i + \frac{(1-\pi_i)}{\rho_{i,hh}}\rho_{i,hh}^k h_i^k(P_{i,0}) + \frac{\pi_i\rho_{i,gh}}{\rho_{i,hh}}\sum_{m=0}^{k-2}\rho_{i,hh}^{m+1}h_i^{m+1}(M_i) \tag{4.17}$$

where $M_i = A_i C_i^{-1} R_i C_i'^{-1} A_i' + Q_i$, Now the first term on the right hand side is finite. From Lemma 4.4.4 the second term is finite as $k \to \infty$ if $\rho_{i,hh}{\alpha_i}^2 < 1$. The third term

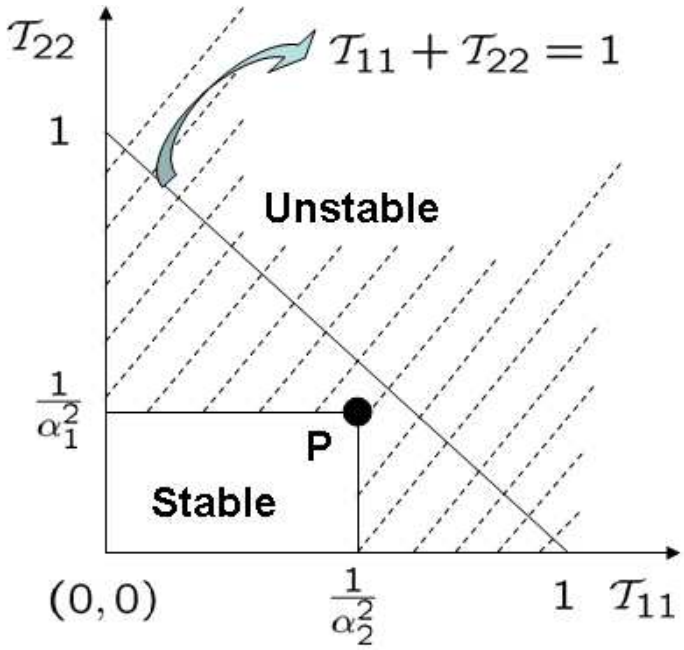

Figure 4.2: S_k is a Markov process, $N = 2$.

after summing the geometric series can be rewritten as

$$\frac{\pi_i \rho_{i,gh}}{\rho_{i,hh}} \left[\sum_{m=1}^{k-1} \tilde{A}_i^m M_i (\tilde{A}_i^m)' + \frac{\rho_{i,hh}}{1-\rho_{i,hh}} \sum_{m=0}^{k-2} \tilde{A}_i^m Q_i (\tilde{A}_i^m)' (1 - \rho_{i,hh}^{k-1-m}) \right], \tag{4.18}$$

where $\tilde{A}_i = \sqrt{\rho_{i,hh}} A_i$. Again using Lemma 4.4.4 we know that this term is finite as $k \to \infty$ if $\rho_{i,hh} {\alpha_i}^2 < 1$. □

Note that for the $N = 2$ case, $\pi_1 = (1 - \mathcal{T}_{22})/(2 - \mathcal{T}_{22} - \mathcal{T}_{11})$ and $\pi_2 = 1 - \pi_1$, where $\mathcal{T}_{ii} \in (0, 1)$ for ergodicity. It can be easily verified using (4.15) that $\rho_{1,hh} = \mathcal{T}_{22}$ and $\rho_{2,hh} = \mathcal{T}_{11}$. Therefore, the instability region from Theorem 4.4.1 is the shaded region in Fig. 4.2. Now a two state Markov chain is an i.i.d. distribution for the case when $\mathcal{T}_{11} + \mathcal{T}_{22} = 1$. Now we can see from Fig. 4.2 that if $1/\alpha_1^2 + 1/\alpha_2^2 < 1$, then point P lies below the line and thus the dynamic coverage problem cannot be solved by an i.i.d. sensor motion algorithm. This shows that Proposition 4.3.1 is a special case of Theorem 4.4.1.

Example 11. *Consider two scalar systems with parameters* $A_1 = 1.25$, $C_1 = 0.2$, $R_1 = 2.5$, $Q_1 = 20$, $A_2 = 1.7$, $C_2 = 0.4$, $R_2 = 2$ *and* $Q_2 = 10$. *The quantity* $1/\alpha_1^2 + 1/\alpha_2^2 = 0.986 < 1$, *therefore an i.i.d. sensor motion strategy will not be able solve the dynamic coverage*

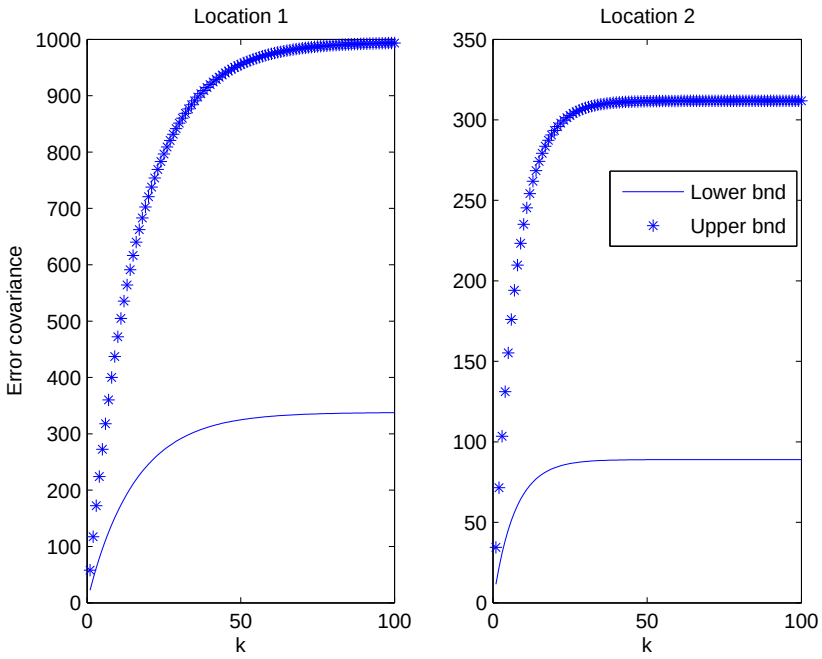

Figure 4.3: Bounds on error covariance.

problem, but a Markov chain strategy with the following transition probability matrix

$$\mathcal{T} = \begin{bmatrix} 0.3 & 0.7 \\ 0.4 & 0.6 \end{bmatrix}$$

solves the coverage problem with the expected error covariance contained between the lower and upper bounds as shown in Fig. 4.3.

4.5 Conclusions and Future Directions

In this chapter I define the dynamic sensor coverage problem. I have considered a simple case in which N spatially separated linear systems whose dynamics are decoupled have to be observed by a single mobile sensor. Due to the finite range of the sensor, it can make measurements for a particular system, only if it happens to be at that system. I have modeled the motion of the sensor as an i.i.d. process and as an ergodic Markov chain.

There are several avenues of research that this chapter opens up. The most immediate

one is the introduction of feedback. It should be noted that even though this chapter gives success and failure bounds on probabilities for random sensor motion algorithms, it does not talk about how to change the motion algorithm based on the uncertainty profile in the space. The question *"Where to move?"* based on the confidence in estimates, requires further analysis. Constructive procedures for an appropriate transition probability matrix, respecting physical motion constraints between spatially separate locations, need to be developed. I have attempted to provide a deterministic answer to this question in the next chapter.

Other research directions that I am currently pursuing are solving the coverage problem when the dynamics of the environment are coupled and dependent at different locations and solving the dynamic coverage problem with multiple sensors.

Chapter 5

Dynamic sensor coverage with uncertainty feedback

5.1 Introduction

Dynamic sensor coverage is a problem of utmost interest for a wide variety of applications. The idea of having a *few, limited range, mobile* sensors perform the coverage task instead of employing multiple static sensors can result in immense savings in resources for almost the same degree of performance. The application areas for this problem can range from design of better and more intelligent surveillance systems, to solving situational awareness problems, to weather monitoring, to search and reconnaissance, and also to sensor networks.

In [45] and in Chapter 4 I presented two stochastic strategies for solving the dynamic sensor coverage problem. Under one strategy the stochastic process defining sensor motion was i.i.d. and in the other it was a Markov chain. I gave success and failure results for both these strategies. Such results were also independently developed in [44]. One ingredient that is lacking in the previous work is that there was no real time control of the sensor motion; in other words, once the surveillance system designer had information about the dynamics of uncertainty at all spatial locations, the sensor motion algorithm was designed off-line and it remained fixed after that. In this chapter I present some simple control strategies and intelligent algorithms to enable the sensor to answer the question of *where to move* based on the current uncertainty profile in space.

I first present a model of our environment, which is exactly similar to the one in chapter 4. This chapter contains results when the environment can be modeled as two spatially separate systems **1** and **2**; however I plan to extend the results to multiple locations and multiple sensors. In this chapter the sensor moves according to the relative uncertainty in the estimates of the states of the linear systems evolving at location **1** and **2**. Error covariance is used as a metric of uncertainty. As in Chapter 4, the sensor uses a Kalman filter to estimate the states of the two systems. It simply predicts when there is no measurement available and corrects when there is a measurement. The error covariance evolves according to the Lyapunov equation and Riccati equation under the prediction and correction steps, respectively. This results in a switched iterated map system (SIMS). We then analyze the ω limit set of the SIMS. In this chapter we present local attractivity result for a unique period two orbit. We also show that this orbit is globally attractive for a scalar special case. We present a few examples to illustrate the concept. Similar problem treatment can be found in [50], however the authors consider scalar systems and are concerned with optimality over a finite epoch. The motivation in the above paper is to optimally switch beam patterns of a phased-array antenna radar in order to track multiple targets.

Most of the results presented in this chapter have been published in [51].

5.1.1 Notation

$\times$	Cartesian product
$\otimes$	Kronecker product
$DF(x)$	Jacobian of function F at point x
$\mathbb{R}$	Real number field
X'	Transpose of an (n, m) real matrix X
tr$[X]$	Trace of an (n, n) real matrix X
$\mathbb{S}_n$	Cone of real (n, n) symmetric positive semidefinite matrices
$\mathbb{S}_n^+$	Cone of real (n, n) symmetric positive definite matrices
$X \geq Y, X > Y$ for $X, Y \in \mathbb{S}_n$	$X - Y \in \mathbb{S}_n, \in \mathbb{S}_n^+$
$f^n(X)$	A function applied n times
int$[\Delta]$	Strict interior of a set Δ
$\lambda[A]$	Set of all eigenvalues of matrix A

5.2 Problem Description

Consider two independently evolving LTI systems **1** and **2**, placed at different locations, whose dynamics are given by

$$\begin{cases} x_{i,k+1} = A_i x_{i,k} + w_{i,k} \\ y_{i,k} = C_i x_{i,k} + v_{i,k} \end{cases}, \tag{5.1}$$

where $x_{i,k}$, $x_{i,k+1}$, $w_{i,k} \in \mathbb{R}^{n_i}$ and $y_{i,k}$, $v_{i,k} \in \mathbb{R}^{m_i}$, $w_{i,k}$ and $v_{i,k}$ are Gaussian random vectors with zero mean and covariance matrices Q_i and R_i, respectively, and i takes values in the set $\{1, 2\}$. $x_{i,0}$ is assumed to be a Gaussian random variable with mean $x_{i,0}$ and covariance matrix $P_{i,0}$ Both process and sensor noises are assumed to be white and independent of each other and of the initial conditions.

The task for the sensor is to provide the best possible estimate of the states of systems

1 and **2** for all time. At a given instance of time the sensor can either be at system **1** or **2**. Due to the limited range constraint the sensor can make measurements only for the system where it is physically present at that time. The sensor executes a standard Kalman filtering algorithm for estimation [52]. The prediction step is always executed for both systems, but the correction step is executed only for the system where the sensor is physically located. Let $I_{i,k}$ be the indicator function describing whether or not the sensor is at location i at time k.

Define the following relations for $X \in \mathbb{S}_n$:

$$h(X) \triangleq AXA' + Q, \tag{5.2}$$

$$f(X) \triangleq AXC'(CXC' + R)^{-1}CXA', \tag{5.3}$$

$$g(X) \triangleq h(X) - f(X). \tag{5.4}$$

In the rest of this chapter $h_i(X)$, $g_i(X)$, and $f_i(X)$ will refer to the same functional forms as described above but with parameters of system i. For example $h_i(X) = A_iXA_i' + Q_i$ for $i \in \{1, 2\}$.

Under the estimation scheme described above the recursion of the error covariance matrices looks like

$$P_{i,k+1} = \begin{cases} h_i(P_{i,k}) & I_{i,k} = 1 \\ g_i(P_{i,k}) & I_{i,k} = 0 \end{cases}. \tag{5.5}$$

Define P_k as

$$P_k \triangleq (P_{1,k}, P_{2,k}) \in \mathbb{S}_{n_1} \times \mathbb{S}_{n_2}. \tag{5.6}$$

Now we are in a position to state the problem description.

For a given model of uncertainty at spatially separate locations (5.1), find a class of sensor motion algorithms that guarantee P_k live in a bounded invariant subset of $\mathbb{S}_{n_1} \times \mathbb{S}_{n_2}$, as $k \to \infty$. Is it possible to find the smallest such invariant subset?

In this chapter we present one class of sensor motion algorithm. We prove local stability of a period two orbit and prove global stability for the scalar case.

5.3 Preliminaries

In this section we will present a series of results, required for our analysis. While stating these preliminary results we will omit the subscript i if the result holds for both values of i.

Lemma 5.3.1. *(a) If A is unstable then*

$$\lim_{k\to\infty} h^k(X_0) = \infty$$

for all $X_0 \in \mathbb{S}_n$.

(b) If the spectral radius of A, $\alpha < 1$, and the pair $(A, \sqrt{Q})$ is observable, then the Lyapunov difference equation $X_{k+1} = h(X_k)$ converges to a unique solution $T \in \mathbb{S}_n^+$ as $k \to \infty$. In other words the following infinite sum

$$\lim_{k\to\infty}\left[A^k X_0 A'^k + \sum_{m=0}^{k-1} A^m Q A'^m\right]$$

is a finite positive definite matrix $T > 0$ for all $X_0 \geq 0$, where $T = h(T)$.

Proof: See [49]. □

Lemma 5.3.2. *If (A, C) is detectable and $(A, \sqrt{Q})$ is stabilizable, then there is a unique $\overline{P} \in \mathbb{S}_n^+$, independent of the initial condition X_0 that is a solution to the Riccati recursion*

$$X_{k+1} = g(X_k),$$

Furthermore, $\overline{P}$ is also the unique positive definite solution to the discrete algebraic Riccati equation (DARE)

$$X = g(X). \tag{5.7}$$

Proof: See [52]. □

Lemma 5.3.3. *If (A^{n+1}, C) is detectable and $(A^{n+1}, \sqrt{\sum_{k=0}^{n} A^k Q A'^k})$ is stabilizable, then there exists a unique positive definite solution to the equation*

$$h^n(g(X)) = X.$$

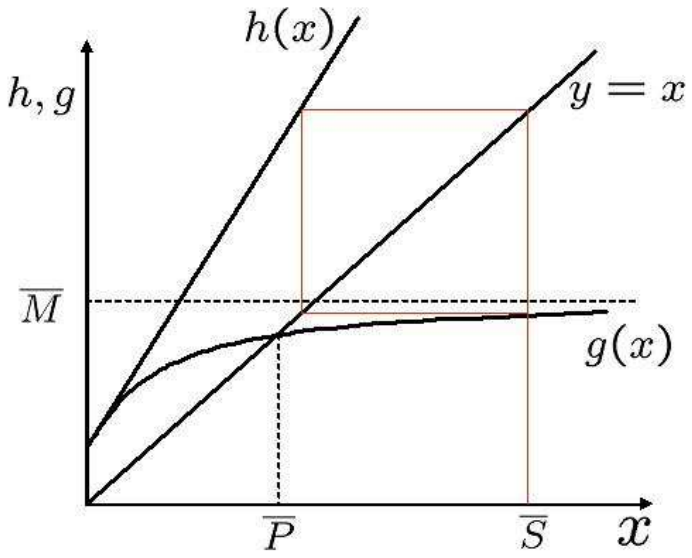

Figure 5.1: Functions $h(X)$ and $g(X)$ in the scalar case with unstable A.

The solution can be found by solving the DARE $\tilde{g}(X) = X$, *with* $\tilde{A} = A^{n+1}$ *and* $\tilde{Q} = \sum_{k=0}^{n} A^k Q A'^k$.

Proof:

$$\begin{aligned} h^n(g(X)) &= A^{n+1}XA'^{n+1} + \sum_{k=0}^{n} A^k Q A'^k - A^{n+1}XC' \\ &\quad \times (CXC' + R)^{-1} CXA'^{n+1}. \end{aligned} \tag{5.8}$$

It's easy to see that the above equation has the same form as eqn. (5.4) with A and Q replaced by A^{n+1} and $\sum_{k=0}^{n} A^k Q A'^k$, respectively. □

Lemma 5.3.4. *The following properties of functions* $g(X)$ *and* $h(X)$ *hold:*

(a) If $X \geq Y$, *then* $g(X) \geq g(Y)$ *and* $h(X) \geq h(Y)$.

(b) If $X \geq Y$ *and for some scalar* $\lambda \in [0, 1]$, $g(\lambda X + (1 - \lambda)Y) \geq \lambda g(X) + (1 - \lambda)g(Y)$.

(c) If C *is invertible, then* $g(X) \leq \overline{M} = AC^{-1}RC'^{-1}A' + Q \; \forall X \in \mathbb{S}_n$.

(d) If a unique solution $\overline{P} \in \mathbb{S}_n^+$ *to the DARE,* $g(X) = X$ *exists, then,*

(i) $h(\overline{P}) \geq \overline{P}$.

(ii) $g(X) \geq \overline{P}, \forall X \geq \overline{P}$.

(iii) $g(X) \leq \overline{P}, \forall X \leq \overline{P}$.

(iv) *If in addition a unique solution* $\overline{T} \in \mathbb{S}_n^+$ *to the Lyapunov equation,* $h(X) = X$ *exists, then* $\overline{T} \geq \overline{P}$.

(v) *If in addition a unique solution* $\overline{S} \in \mathbb{S}_n^+$ *to the DARE,* $hg(X) = X$ *exists, then,* $\overline{S} \geq \overline{P}$.

(vi) *If both unique* $\overline{T} \in \mathbb{S}_n^+$ *and* $\overline{S} \in \mathbb{S}_n^+$ *exist, then* $\overline{T} \geq \overline{S}$.

Proof: For (a), (b) see [46]. For (c) see [45].

(d) (i) $\overline{P} = g(\overline{P}) = h(\overline{P}) - f(\overline{P})$, $f(\overline{P}) \in \mathbb{S}_n$, therefore $h(\overline{P}) \geq \overline{P}$.

(ii) By (a) and the definition of $\overline{P}$.

(iii) By (a) and the definition of $\overline{P}$.

(iv) Consider the set $\mathbb{D} = \{X \in \mathbb{S}_n : X \geq \overline{P}\}$. $\mathbb{D}$ is invariant under the map $h(X)$. Choose $X_0 \in \mathbb{D}$ then by Lemma 5.3.1 (b), we have $\lim_{k\to\infty} h^k(X_0) = \overline{T} \in \mathbb{D}$. Hence $\overline{T} \geq \overline{P}$.

(v) Recall set $\mathbb{D}$ from (iv). From (a) and (d)(i), we know that $\mathbb{D}$ is invariant under the maps $h(X)$ and $g(X)$. By Lemma 5.3.3 we know that $hg(X) = X$ is an algebraic Riccati equation. Therefore by Lemma 5.3.2, repeated application of $hg(X)$ on some initial condition in the set $\mathbb{D}$ will result in the solution $\overline{S}$. In other words, if $X_0 \in \mathbb{D}$ then $\overline{S} = \lim_{k\to\infty} (hg)^k(X_0) \in \mathbb{D}$, hence $\overline{S} \geq \overline{P}$.

(vi) From equations (5.2), (5.3), and (5.4) we know $h(X) \geq g(X)$. This implies using increasing property of $h(X)$, $\overline{T} = \lim_{k\to\infty} h^k(X_0) \geq \lim_{k\to\infty} (hg)^k(X_0) = \overline{S}$.

□

Lemma 5.3.5. *Given* $X = X'$, *then* $X \in \mathbb{S}_n$ *iff* $\forall Y \in \mathbb{S}_n$, $tr[YX] \geq 0$.

Proof: *(Necessity.)* If $X, Y \in \mathbb{S}_n$, then by trace of the product inequality [49] $\lambda_{min}(X)tr[Y] \leq tr[XY] \leq \lambda_{max}(X)tr[Y]$, where $\lambda_{min}(X)$ and $\lambda_{max}(X)$ are the minimum and maximum eigenvalues of X. Since $X, Y \in \mathbb{S}_n$, all their eigenvalues are non-negative real numbers. Thus $tr[XY] \geq 0$.

(Sufficiency.) Given $tr[XY] \geq 0, \forall Y \in \mathbb{S}_n$ and $X = X'$. This implies $tr[Xyy'] \geq 0$, for all $y \in \mathbb{R}^n$. But $tr[Xyy'] = tr[y'Xy]$, therefore $y'Xy \geq 0$. Thus $X \in \mathbb{S}_n$. □

Lemma 5.3.6. *If a unique solution $\overline{P}$ to the DARE $g(X) = X$ exists, then for all $X > \overline{P}$, there exists $\Gamma \in \mathbb{S}_n$, such that $tr[\Gamma X] > tr[\Gamma g(X)]$.*

Proof: Proof by contradiction. Let there exist $X_0 > \overline{P}$, such that $\forall \Gamma \in \mathbb{S}_n$, $\text{tr}[\Gamma X_0] \leq \text{tr}[\Gamma g(X_0)]$. Therefore by Lemma 5.3.5 $X_0 \leq g(X_0)$. Now using Lemma 5.3.4 $g^k(X_0) \leq g^{k+1}(X_0)$, therefore $\lim_{k\to\infty} g^k(X_0) \neq \overline{P}$, which is a contradiction to Lemma 5.3.2. □

Remark 5.3.1. *One can prove a similar result $\forall X < \overline{P}$; there exists a $\Gamma \in \mathbb{S}_n$ such that $tr[\Gamma X] < tr[\Gamma g(X)]$. These results are not too surprising as they are a manifestation of the concavity property of $g(X)$. In the scalar case the above result suggests $X > g(X)$ if $X > \overline{P}$ and $X < g(X)$ if $X < \overline{P}$, which is always true for concave functions. See fig. 5.1.*

Let $\mathcal{E}$ be the family of all functions formed by taking the compositions of $h(X)$ and $g(X)$ in any order. In other words,

$$\mathcal{E} = \{h, g, hg, gh, g^2, h^2, hg^2, ghg \cdots\}. \tag{5.9}$$

Lemma 5.3.7. *All functions $e(X) \in \mathcal{E}$ are concave and increasing:*

(a) If $X \geq Y$, then $e(X) \geq e(Y)$.

(b) If $X \geq Y$ and for a scalar $\lambda \in [0, 1]$, $e(\lambda X + (1 - \lambda)Y) \geq \lambda e(X) + (1 - \lambda)e(Y)$.

Proof: Follows easily from Lemma 5.3.4 and

$$h(\lambda X + (1 - \lambda)Y) = \lambda h(X) + (1 - \lambda)h(Y), \quad \forall \lambda \in [0, 1].$$

□

5.4 Procedure

I now give a step by step procedure to partition the uncertainty space $\mathbb{S}_{n_1} \times \mathbb{S}_{n_2}$ into two regions. Based on which partition the overall uncertainty lies in, the sensor decides to move

to location **1** or **2**. After each step we prove its feasibility of execution using results from Section 5.3. In the rest of the chapter we assume that the following assumption holds:

Assumption(*): (A_i^2, C_i) is detectable and $(A_i^2, \sqrt{A_i Q_i A_i' + Q_i})$ is stabilizable for $i \in \{1, 2\}$.

Remark 5.4.1. *Note that we do not require the matrices A_i to be stable.*

[Step 1] In this step we find a two period cycle, for the case when the sensor keeps oscillating between locations **1** and **2**. Lets first state the following result.

Proposition 5.4.1. *If assumption(*) holds and if the sensor keeps oscillating between location* **1** *and* **2***, then P_k converges to a unique two period cycle C as $k \to \infty$. The periodic points of the limit cycle are given by*

$$\mathcal{P}_1 = (\overline{S}_1, g_2(\overline{S}_2)), \text{ and } \mathcal{P}_2 = (g_1(\overline{S}_1), \overline{S}_2), \tag{5.10}$$

where $\overline{S}_1$ and $\overline{S}_2$ are unique positive definite solutions to the equations

$$X = h_1 g_1(X), \text{ and } X = h_2 g_2(X),$$

respectively.

Proof: If the sensor keeps oscillating between location **1** and **2** then the error covariance evolves as

$$\cdots \mathcal{F}_{\Delta_1} \mathcal{F}_{\Delta_2} \mathcal{F}_{\Delta_1} \mathcal{F}_{\Delta_2}(P_0),$$

where

$$\mathcal{F}_{\Delta_1}(P_k) \stackrel{\triangle}{=} \begin{pmatrix} g_1(P_{1,k}) \\ h_2(P_{2,k}) \end{pmatrix}, \tag{5.11}$$

$$\mathcal{F}_{\Delta_2}(P_k) \stackrel{\triangle}{=} \begin{pmatrix} h_1(P_{1,k}) \\ g_2(P_{2,k}) \end{pmatrix}. \tag{5.12}$$

Now from Lemma 5.3.3 $hg(X) = X$ is a DARE and by Lemma 5.3.2 it has a unique solution under assumption(*). If the sensor keeps switching between the two locations, it's

equivalent to repeated application of the map $hg(X)$, hence the trajectories converge to C. □

From Lemma 5.3.3 we know that $\overline{S}_i$ are unique and can be found by solving the DARE. Thus its possible to analytically solve for the periodic points.

[Step 2] In this step we will find a separating hyperplane between the periodic points $\mathcal{P}_1$ and $\mathcal{P}_2$ found in **[Step 1]**.

Proposition 5.4.2. *If assumption(*) holds, then there exists a separating hyperplane between points $\mathcal{P}_1$ and $\mathcal{P}_2$.*

Proof: From Lemma 5.3.4(d)(v) we know that $\overline{S}_2 \geq \overline{P}_2$; therefore, from Lemma 5.3.6 we know that there exists a $\Gamma_2 \in \mathbb{S}_n$ and a scalar $\zeta > 0$ such that

$$\text{tr}[\Gamma_2 \overline{S}_2] > \zeta \quad ; \quad \text{tr}[\Gamma_2 g_2(\overline{S}_2)] < \zeta. \tag{5.13}$$

Thus we have found a separating hyperplane $\text{tr}[\Gamma_2 X] = \zeta$ between points $\mathcal{P}_1$ and $\mathcal{P}_2$. □

Remark 5.4.2. *The condition in eqn. (5.13) is linear in Γ_2 and ζ_2 and a feasible hyperplane can be easily computed.*

Remark 5.4.3. *The most general equation of a hyperplane in $\mathbb{S}_{n_1} \times \mathbb{S}_{n_2}$ is*

$$tr[\Gamma_1 X_1] + tr[\Gamma_2 X_2] = \zeta,$$

where $X_i \in \mathbb{S}_{n_i}$, Γ_1, Γ_2 are real symmetric matrices and ζ is a scalar.

We now define the following two exhaustive and mutually exclusive partitions of $\mathbb{S}_{n_1} \times \mathbb{S}_{n_2}$,

$$\Delta_1 = \{(X_1, X_2) \in \mathbb{S}_{n_1} \times \mathbb{S}_{n_2} \quad : \quad \text{tr}[\Gamma_2 X_2)] < \zeta\}, \tag{5.14}$$

$$\Delta_2 = \{(X_1, X_2) \in \mathbb{S}_{n_1} \times \mathbb{S}_{n_2} \quad : \quad \text{tr}[\Gamma_2 X_2)] \geq \zeta\}. \tag{5.15}$$

Remark 5.4.4. *By definition of Δ_1 and Δ_2, $\mathcal{P}_1 \in \Delta_1$ and $\mathcal{P}_2 \in \Delta_2$.*

[Step 3] In this step we use the separating hyperplane found in **[Step 2]** to present the following motion control algorithm for the sensor:

(i) Start with initial error covariance matrix pair $P_0 = (P_{1,0}, P_{2,0})$.

(ii) If $P_k \in \Delta_1$, then go to location **1**, else go to location **2** at time $k + 1$.

(iii) $k = k + 1$, go to step (ii).

Therefore at time k, the dynamics in the $\mathbb{S}_{n_1} \times \mathbb{S}_{n_2}$ space iterates according to the following map:

$$P_{k+1} = \begin{cases} \mathcal{F}_{\Delta_1}(P_k), & P_k \in \Delta_1 \\ \mathcal{F}_{\Delta_2}(P_k), & P_k \in \Delta_2 \end{cases} . \tag{5.16}$$

The algorithm above describes a switched iterated maps system (SIMS). There is a discontinuity at the separating hyperplane. Our objective is to prove the global stability of the period two orbit C. In this chapter we prove local stability of the periodic orbit C for the general case. We prove global stability for the scalar case.

Similar results have been shown to hold in the case of switched server systems [53] and the references therein. However, the dynamics are assumed to be linear in all the existing results. In the case presented in this chapter $g(X)$ is a non-linear map. In [54] the author talks about iterated function systems with an assumption of continuity, and all maps are assumed to be contractive. In our case, since we allow unstable A_i's the map $h(X)$ need not be contractive and there can be discontinuity at the separating hyperplane.

5.5 Results for the Switched Iterated Map System

We start this section with a couple of easily provable results.

Theorem 5.5.1. *If the sensor moves according to the algorithm described in Section 5.4 , then for every initial covariance pair $P_0 \in \mathbb{S}_{n_1} \times \mathbb{S}_{n_2}$, and for every $k_s s > 0$, there exist time instants $k_1, k_2 > k_s s$, such that $P_{k_1} \in \Delta_1$ and $P_{k_2} \in \Delta_2$.*

Proof: Proof by contradiction. Let there exist an initial condition P_0 for which there exists a $k_s s > 0$, such that $P_k \in \Delta_1$, for all $k > k_s s$. Thus map h_2 is applied to $P_{2,k}$ at every

instant after $k_s s$. Now if A_2 is stable, a unique $\overline{T}_2$ exists and $\lim_{k\to\infty} h_2^k(P_{2,0}) = \overline{T}_2$. Now since $\overline{T}_2 \geq \overline{S}_2$ by Lemma 5.6.1, therefore using eqn. (5.13) and Lemma 5.3.5 we know that the surface $X_2 = \overline{T}_2$ lies entirely in Δ_2. This is a contradiction.

For the case when A_2 is unstable, from Lemma 5.3.1 the solution to the Lyapunov equation does not exist. Now $\lim_{2k\to\infty} \mathrm{tr}[\Gamma_2 h_2^{2k}(P_{2,0})] \geq \lim_{k\to\infty} \mathrm{tr}[\Gamma_2 (h_2 g_2)^k (P_{2,0})]$ using $h(X) \geq g(X)$ and lemma 5.3.5. But $\lim_{k\to\infty} \mathrm{tr}[\Gamma_2 (h_2 g_2)^k (P_{2,0})]$ approaches $\mathrm{tr}[\Gamma_2 \overline{S}_2]$, which is a value greater than ζ. Therefore eventually the covariance pair evolves into Δ_2, which is a contradiction.

Similarly one can arrive at a contradiction if the covariance pair is assumed to be constrained within Δ_2. □.

The following corollary follows immediately:

Corollary 5.5.1. *There does not exist a fixed point in $\mathbb{S}_{n_1} \times \mathbb{S}_{n_2}$. There does not exist a limit cycle in $\mathbb{S}_{n_1} \times \mathbb{S}_{n_2}$, all of whose periodic points lie in Δ_1 or Δ_2.*

In the rest of this section we prove that the two period orbit C is locally attracting.

We first define the notion of local attractivity of periodic points.

Definition 5.5.1. *Consider a map $F : \mathbb{R}^n \to \mathbb{R}^n$ with period m, i.e., $F^m(p) = p$, where $p \in \mathbb{R}^n$ is one of the periodic points. p is called a locally attracting periodic point, if there exists an open set about p in which all points tend to p under forward iterations of F.*

The following facts to check local attractivity are well known [55].

Fact 5.5.1. *p is a locally attracting periodic point if all of the eigenvalues of $DF^m(p)$ are less than* 1 *in absolute value.*

Fact 5.5.2. *For periodic orbits, the eigenvalues of the Jacobian matrix of F^m are same at each periodic point of the orbit. In other words $\lambda[DF^m(F^j(p))]$ are the same for $j \in \{0, 1, 2 \cdots m-1\}$.*

So in order to prove local attractivity of the periodic orbit C it's enough to show that all eigenvalues of the Jacobian matrix of the two step map $\mathcal{F}_{\Delta_2}\mathcal{F}_{\Delta_1}$ evaluated at the point $\mathcal{P}_1$ lie inside the unit circle. The Jacobian matrix $D[\mathcal{F}_{\Delta_2}\mathcal{F}_{\Delta_1}(x)]|_{x=\mathcal{P}_1}$ can be written as

$$\begin{bmatrix} \frac{d(h_1 g_1(X_1))}{dX_1}|_{X_1=\overline{S}_1} & 0 \\ 0 & \frac{d(g_2 h_2(X_2))}{dX_2}|_{X_2=g_2(\overline{S}_2)} \end{bmatrix}. \tag{5.17}$$

Since the Jacobian matrix does not have any cross terms, its eigenvalues are the eigenvalues of the diagonal terms. Let us consider the first diagonal term. The following equation can be derived using the matrix differentiation section in [56]:

$$\frac{d(h_1 g_1(X_1))}{dX_1}|_{X_1=\overline{S}_1} = \Omega_1 \otimes \Omega_1, \tag{5.18}$$

where

$$\Omega_1 = A_1^2 - A_1^2 \overline{S}_1 C_1' (C_1 \overline{S}_1 C_1' + R_1)^{-1} C_1. \tag{5.19}$$

Now the eigenvalues of $\Omega_1 \otimes \Omega_1$ are the products of all possible pairs of eigenvalues of Ω_1 [57]. So in order to prove that the eigenvalues of $\Omega_1 \otimes \Omega_1$ are inside the unit circle, it's enough to show that the eigenvalues of Ω_1, are all of modulus less than 1.

Under assumption(*) and using Lemma 5.3.3, we know that a unique solution $\overline{S}_1 \in \mathbb{S}_n^+$ to the DARE $h_1 g_1(X) = X$ exists, therefore a stable Kalman filter for the LTI system

$$\begin{aligned} x_{k+1} &= A_1^2 x_k + w_k \quad w_k \sim \mathcal{N}(0, A_1 Q_1 A_1' + Q_1), \\ y_k &= C_1 x_k + v_k \quad v_k \sim \mathcal{N}(0, R_1) \end{aligned} \tag{5.20}$$

can be found. The matrix $K_k = A_1^2 \overline{S}_1 C_1' (C_1 \overline{S}_1 C_1' + R_1)^{-1}$ is the corresponding Kalman gain and the error dynamics are given by

$$e_{k+1} = \Omega_1 e_k + w_k - K_k v_k. \tag{5.21}$$

But since the Kalman filter is stable, all eigenvalues of Ω_1 must be strictly inside the unit circle.

Let us now look at the second diagonal entry of the Jacobian matrix, and using fact 5.5.2

$$\lambda \left[\frac{d(g_2 h_2(X_2))}{dX_2}|_{X_2=g_2(\overline{S}_2)} \right] = \lambda \left[\frac{d(h_2 g_2(X_2))}{dX_2}|_{X_2=\overline{S}_2} \right]. \tag{5.22}$$

Using a similar line of reasoning, we know that all eigenvalues of $d(g_2h_2(X_2))/dX_2|_{X_2=g_2(\overline{S}_2)}$ are inside the unit circle. Therefore, the periodic orbit C is locally attracting.

Remark 5.5.1. *The proof of local attractivity is independent of the separator found in Section 5.4* **[Step 2]**. *The proof holds as long as* $\mathcal{P}_1 \in int[\Delta_1]$ *and* $\mathcal{P}_2 \in int[\Delta_2]$.

5.6 Scalar Case

In this section, we consider the case when the sensor moves between two scalar systems. P_k takes values in the closed positive quadrant of $\mathbb{R}^2$. In the scalar case assumption(*) is equivalent to $C_i \neq 0$.

In addition to Lemma 5.3.4, there are a few additional properties of the maps that hold for the scalar case

Lemma 5.6.1. *Given assumption(*), then for* $X \in \mathbb{S}_1$, *every function* $e(X) \in \mathcal{E}$ *is one-one and strictly increasing. There exists a unique* $\overline{E} > 0$ *such that* $e(\overline{E}) = \overline{E}$. *In addition the concavity of* $e(X)$ *implies* $X > \overline{E} \Leftrightarrow e(X) < X$.

Proof of the lemma follows using concavity of functions and is left for the reader to verify.

The separator in this case will be any line $X_2 = c_2$, such that $g_2(\overline{S}_2) < c_2 < \overline{S}_2$. The partition Δ_1 is the region $X_2 < c_2$. Note that $h_i(X_i)$ are invertible in the scalar case. Define the following two regions in $\mathbb{S}_1 \times \mathbb{S}_1$:

$$\kappa_1 = \{X : h_2^{-1}(c_2) \leq X_2 < c_2\}, \tag{5.23}$$

$$\kappa_2 = \{X : c_2 \leq X_2 < g_2^{-1}(c_2)\}. \tag{5.24}$$

κ_1, κ_2 are the sets of all those points in Δ_1, Δ_2 that map to the region Δ_2, Δ_1 in one time step.

By Theorem 5.5.1 we know that all trajectories that originate in Δ_1 will eventually switch to Δ_2 and vice versa.

All $X \in \kappa_1$ map to a set entirely contained in κ_2

$$c_2 \leq h_2(X_2) < h_2(c_2) < g_2^{-1}(c_2), \tag{5.25}$$

where the last inequality follows using Lemma 5.6.1 and noting that c_2 is greater than the fixed point $g_2(\overline{S}_2)$ of the function $g_2 h_2$.

Similarly, all $X \in \kappa_2$ map to a set entirely contained in κ_1. This implies that all trajectories will eventually switch back and forth between κ_1 and κ_2 and thus they will all converge to the period two limit cycle C using a similar reasoning as in the proof of proposition 5.4.1.

Remark 5.6.1. *We strongly believe that under the sensor motion algorithm described in Section 5.4, the orbit C is globally stable in the general non-scalar case. We are currently working on the proof for this case.*

5.7 Examples

Consider two systems with

$$A_1 = \begin{bmatrix} 1.25 & 0 \\ 1 & 1.1 \end{bmatrix} \quad A_2 = \begin{bmatrix} 1.01 & 0 \\ 2 & 0.8 \end{bmatrix}$$

$$C_1 = \begin{bmatrix} 1 & 1 \end{bmatrix} \quad C_2 = \begin{bmatrix} 1 & 1 \end{bmatrix}$$

$$Q1 = \begin{bmatrix} 1 & 0 \\ 0 & 1 \end{bmatrix} \quad Q_2 = \begin{bmatrix} 1 & 0 \\ 0 & 2 \end{bmatrix}$$

$$R_1 = 2.5 \quad R_2 = 1.5$$

Assumption(*) is satisfied therefore for this system, thus we can find unique

$$\overline{S}_1 = \begin{bmatrix} 6.7565 & 6.1546 \\ 6.1546 & 11.5178 \end{bmatrix}, \quad \overline{S}_2 = \begin{bmatrix} 3.0213 & 5.1904 \\ 5.1904 & 17.8453 \end{bmatrix}$$

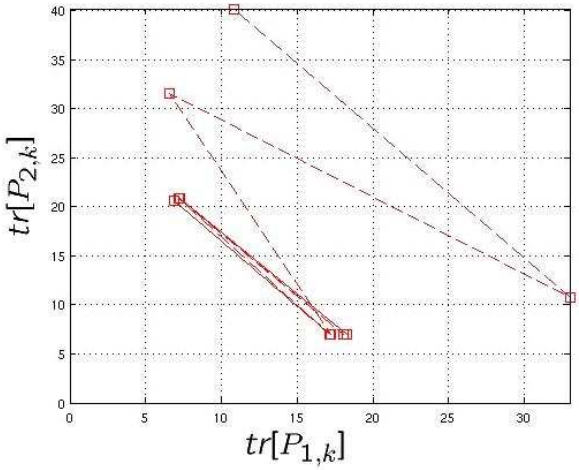

Figure 5.2: Convergence to C.

by solving the DARE. A separating hyperplane can then be found by solving the convex feasibility conditions (5.13).

$$\text{tr}\left(\begin{bmatrix} 0.8009 & -0.19 \\ -0.19 & 0.1991 \end{bmatrix} X_2\right) = 3.014$$

Using the sensor motion algorithm described in Section 5.4 **[Step 3]**, the trajectories of the SIMS, converge to orbit C. Figure 5.2 shows evolution of the trace of X_1 and X_2 starting at a randomly chosen initial condition.

Now let's change ζ in the separating hyperplane to 4.5 instead of 3.014. Note that by doing this condition (5.13) is violated. The resulting trace plot of uncertainties for the same initial conditions is shown in fig. 5.3. The important thing to note is that the steady state behavior is a three period cycle now. Therefore for different partitions of the uncertainty space different steady state sensor schedules can result. For the first partition in this example the sensor took measurements in the order **121212**$\cdots$. For the altered partition the sensor schedule becomes **112112112**$\cdots$. Characterization of the steady state sensor schedules with changing partitions is a future research topic I am exploring right now. For illustration purposes consider the following example:

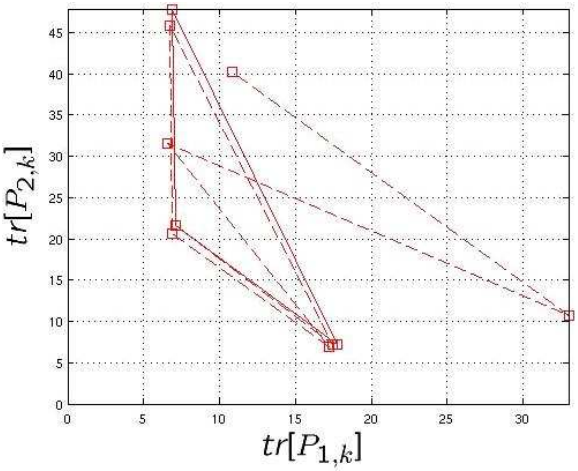

Figure 5.3: Convergence to a three period cycle.

Example 12. *Consider the following two identical systems:*

$$1 : A_1 = 1.4; R_1 = 0.2; Q_1 = 0.4; C_1 = 0.4,$$

$$2 : A_2 = 1.4; R_2 = 0.2; Q_2 = 0.4; C_2 = 0.4.$$

I chose a linear partition passing through the origin with varying slopes and analyze the steady state locations of periodic points. With varying slopes of this partition I get different steady state behavior with different periods. This is shown in fig. 5.4, on the y axis I plot the values of the error covariances of system 1 in steady state. It can be observed that the steady state period is 2, when the partition has slope close to unity. The period increases when the slope of the partition is moved away from unity. It may be now be useful to recall that it was proven in [50] that the optimal sensor scheduling algorithm is obtained with the partition at unity slope.

5.8 Uncertainty feedback: how it helps

We found out in the earlier sections that given full knowledge of system parameters, and following the algorithm developed in Section 5.4, eventually the sensor keeps switching back and forth between **1** and **2**. One may argue that if we know the steady state sensor

motion behavior under this feedback scheme, then why not just hard code the sensor to follow the steady state behavior in an open-loop manner. The question then is what does adding feedback buy us? One immediate answer to this question is that the transient response of convergence to the steady state periodic behavior will be better with feedback. In this section we demonstrate the utility of feedback by considering systems with time varying parameters.

Consider the following scenario in a radar selective beam-forming example. Let there be two different targets that the radar has to track. Let's assume that target **1** keeps switching between two modes 1_f and 1_s periodically. The dynamics in the modes are given by

$$1_s : A_{1_s} = 1.1; R_{1_s} = 0.2; Q_{1_s} = 0.1; C_{1_s} = 1,$$

$$1_f : A_{1_f} = 1.1; R_{1_f} = 0.2; Q_{1_f} = 0.1; C_{1_f} = 2.$$

Note that C_{1_f} is greater than C_{1_s}. In other words target **1** is more observable in mode 1_f than in 1_s. Let the dynamics of second target be given by

$$A_2 = 1.1; R_2 = 0.2; Q_2 = 0.1; C_2 = 1.$$

Consider the dotted and the solid schedules depicted in fig. 5.5. In the solid schedule the radar measures target **1** when it is in mode 1_f, while in the dotted schedule it measures target **1** when in mode 1_s. An intelligent first guess may suggest that the solid schedule may have lower uncertainty than the dotted schedule because it measures target **1** when it is in the faster mode. Even though this turns out to be true for this example, the choice of the best possible schedule in terms of the steady state uncertainty may not always be as obvious. Later we will present some examples that illustrate this fact.

In this example the radar can end up in two different period two limit cycles on the uncertainty space, corresponding to the solid and dotted schedules in figure 5.5. The steady state limit cycle depends on the initial uncertainty and the initial mode of target **1**. Consider fig. 5.6. If the sensor motion control law is activated when target **1** is in the slow mode and the initial uncertainty lies below the horizontal partition, the trajectory is depicted by

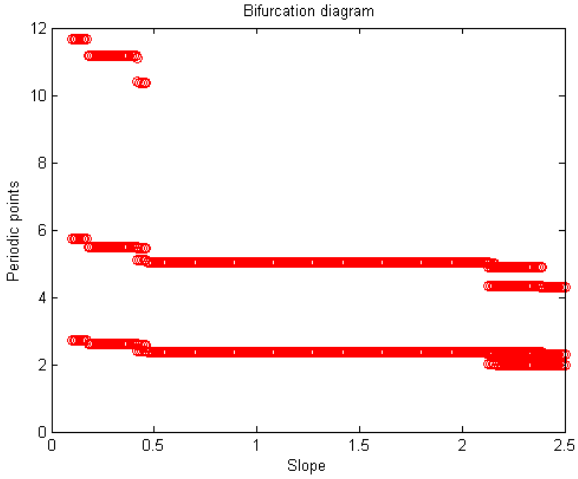

Figure 5.4: Bifurcation Diagram.

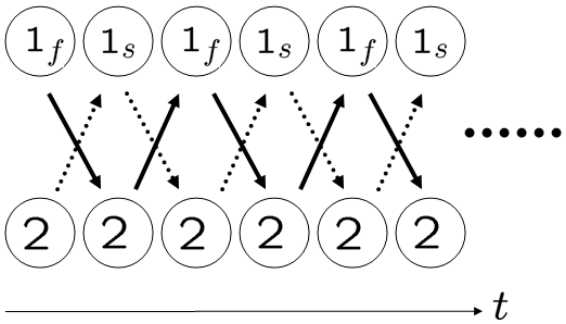

Figure 5.5: Two possible period two steady state sensor schedules.

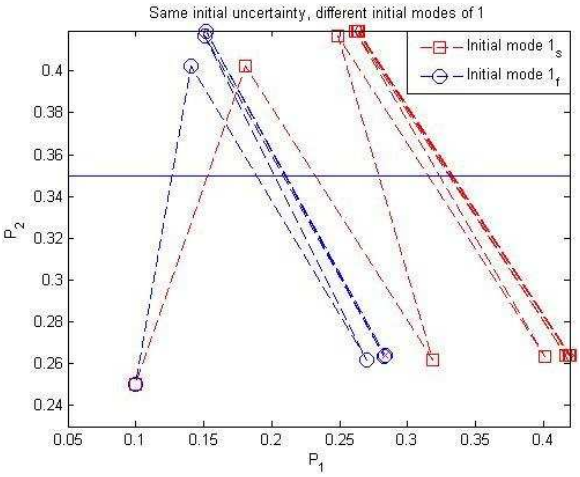

Figure 5.6: Same initial uncertainty profile but target 1 is in different initial modes

rectangles. For the same initial uncertainty, if the motion control law is activated when the target **1** is in the fast mode, the resulting trajectory is represented by circles. Note that the steady state uncertainty is much lower in the later case. Now consider fig. 5.7; even though at time zero, target **1** starts in mode 1_f for both trajectories but the trajectory with iterates represented by circles measures target **1** in the more observable mode. Thus the circle trajectory settles in lower steady state uncertainty.

To illustrate this mathematically we analyze the steady state solutions corresponding to the solid and dotted schedules. The steady state error covariance of target **1**, corresponding to the solid schedule, keeps switching between $\overline{S}_{1,sf}$ and $g_{1,f}(\overline{S}_{1,sf})$, where $\overline{S}_{1,sf}$ is the unique positive definite solution to the equation $h_{1,s}g_{1,f}(X) = X$.

The dotted schedule results in steady state uncertainty of $\overline{S}_{1,fs}$ and $g_{1,s}(\overline{S}_{1,fs})$, where $\overline{S}_{1,fs}$ is the unique positive definite solution to the equation $h_{1,f}g_{1,s}(X) = X$.

Now recall the DARE (5.7) can be rewritten in scalar case as

$$c^2x^2 - x((a^2-1)r + c^2q) - rq = 0. \tag{5.26}$$

The unique positive solution to the above equation is given by

$$x = \frac{(a^2-1)r}{2c^2} + \frac{q}{2} + \sqrt{\frac{(a^2-1)^2r^2}{4c^4} + \frac{q^2}{4} + \frac{rq(a^2+1)}{2c^2}}.$$

From Lemma 5.3.3, we know $h_{1,s}g_{1,f}(X) = X$ is a DARE with $a = A_{1_s}A_{1_f}$, $c = C_{1_f}$, $q = A_{1_s}Q_{1_f}A_{1_s} + Q_{1_s}$ and $r = R_{1_f}$ in eqn. (5.26). Similarly $h_{1,f}g_{1,s}(X) = X$ is a DARE with $a = A_{1_f}A_{1_s}$, $c = C_{1_s}$, $q = A_{1_f}Q_{1_s}A_{1_f} + Q_{1_f}$ and $r = R_{1_s}$ in eqn. (5.26)

For the example considered in this section we have $C_{1,f} > C_{1,s}$. Using this property it is easy to show $\overline{S}_{1,sf} < \overline{S}_{1,fs}$ and $g_{1,f}(\overline{S}_{1,sf}) < g_{1_s}(\overline{S}_{1,fs})$. This proves the lower steady state uncertainty of the solid schedule in fig. 5.5.

Now imagine an open-loop sensor motion control law, where the sensor measures targets **1** and **2** in alternate time instants without using any knowledge of what the relative uncertainty in estimates is and which mode target **1** is in. It is easy to imagine a situation where the sensor can end up in the steady state limit cycle with higher error covariances.

Although if the sensor uses uncertainty feedback and the knowledge of the active mode of target **1**, the following modified sensor motion law always attains the limit cycle with lower error covariance for the particular example of this section.

Algorithm 1.

- *If the uncertainty lies in region* Δ_1 *and,*
  - *Target* **1** *is in mode* 1_f*, then measure target* **1** *else measure target* **2**.
- *If the uncertainty lies in region* Δ_2 *and,*
  - *Target* **1** *is in mode* 1_f*, then measure target* **1**, *else measure target* **2**.

In fig. 5.8 we compare the performance of the above algorithm with a simple open-loop sensor scheduling solution, where the sensor chooses to measure targets **1** and **2** in alternate time intervals. Even though in the first step the above algorithm measures target **1** in spite of the uncertainty being above the partition, it eventually settles down in a lower steady state uncertainty limit cycle. On the other hand, even though at the first step the open-loop algorithm seems to make the right decision but it ends up in a limit cycle with higher uncertainty. This is because the open-loop algorithm is ill-synchronized and measures target **1** when it is in the less observable mode, and since it is open loop it has no way to correct this synchronization.

5.9 Conclusions and Future Directions

This chapter presents an analysis of the sensor coverage problem with uncertainty feedback using iterated Lyapunov and Riccati maps. The sensor motion is based purely on where the overall uncertainty of estimates of various systems lies on the uncertainty space. I have discussed how to partition the space appropriately to obtain a locally stable steady state orbit. I believe that this orbit is also globally stable; however, I do not have the proof of global stability at this moment. In this chapter I presented the proof of global stability for a scalar special case.

This chapter opens up a plethora of interesting research directions. Proving global stability of the two period orbit is an immediate avenue of research. As noted in the example,

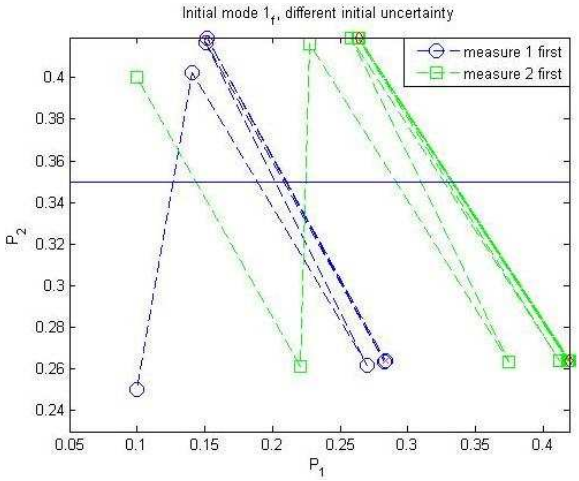

Figure 5.7: Target 1 starts in the same mode, but different initial uncertainty profile

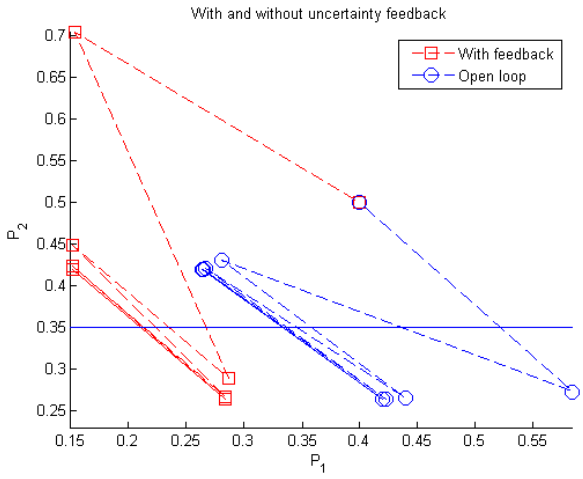

Figure 5.8: Uncertainty feedback helps settle on a lower steady state uncertainty

there needs to be a sound theory for the dependence of the period of the steady state cycle on the separator chosen. Even though in this chapter I always chose a hyperplane as a separator, I believe there exists a class of manifolds that will produce the same kind of steady state behavior. I believe that the theory developed in this chapter will lead to interesting insight into real time algorithms for sensor scheduling and sensor coverage problems.

Chapter 6

Conclusions, extensions, and open questions

This thesis is an illustration of the application of geometric methods for analysis of spatio-temporal planning problems. I have considered a couple of specific problems, the multi-agent rendezvous problem and the dynamic sensor coverage problem. Through these problems I have made an attempt to capture the cooperation and task scheduling constraints of multi-agent planning problems. These constraints have been represented and analyzed on an appropriate space.

Cone invariance is established as the analysis tool for cooperation constraints and has been used in particular to provide certificates for the successful solution of the rendezvous problem. For the sensor coverage problem I have identified the joint space of error covariances as the appropriate space for representation of constraints. I refer to this as the uncertainty space. Decisions on what to measure are made based on where the relative uncertainty lies on this space. In Chapter 4 I present stochastic sensor motion strategies for the sensor coverage problem. The metric chosen there is the expected error covariance.

Controller synthesis for rendezvous based on cone invariance ideas is an open problem and there is ongoing effort in this direction. In [41] the authors analyze the rendezvous synthesis problem in the presence of uncertainty using quadratic cones. The representation of cooperation constraints on the phase plane for other planning problems like interception-evasion and multi-agent consensus is an exciting avenue of research. Generalization of the level set method, as outlined in Chapter 2, to generate control Lyapunov functions for

higher dimensions needs to be investigated.

One can get a lot of new insights into sensor scheduling and coverage algorithms by employing the iterated map analysis presented in this thesis. I have just begun to scratch the surface in this direction, but I strongly believe that the iterated map analysis can help in answering open questions about optimal algorithms. Different steady state periodic orbits on the uncertainty plane and their respective stability properties.

There is some ongoing debate on the efficacy of stochastic algorithms, as presented in Chapter 4, and the deterministic algorithms, as presented in Chapter 5, for sensor coverage tasks. While it turns out that stochastic algorithms may be better suited for a tracking application when the agent to be tracked is adversary and adaptive to any deterministic strategy, for applications like weather monitoring, oceanography, surveillance, and situational awareness deterministic algorithms work better. One interesting question to investigate is the efficacy of fuzzy strategies for coverage tasks.

In [58] the authors have made an attempt to choose the best possible Markov chain describing sensor motion, which results in the lowest steady state expected covariance. The authors used a scatter search hueristic in the above work to come up with different candidate Markov chain transition matrices. Finding an optimal stochastic algorithm is an interesting avenue of future research.

Bibliography

[1] F. Marc, I. Degirmenciyan-Cartault, and A. E. Fallah-Seghrouchni, "Multi-Agent Planning as a Coordination Model for Self-Organized Systems," *Proceeding of the IEEE/WIC International Conference on Intelligent Agent Technology*, 2003.

[2] C. L. Pape, "A Combination of Centralized and Distributed Methods for Multi-agent Planning and Scheduling," *Proceeding of the International Conference of Robotics and Automation*, 1990.

[3] H. Chu and H. A. ElMaraghy, "Real-Time Multi-Robot Path Planner Based on a Heuristic Approach," *Proceeding of the International Conference of Robotics and Automation*, 1992.

[4] A. Mouaddib, "Collective Multi-Objective Planning," *Proceeding of the IEEE Workshop on Distributed Intelligent Systems: Collective Intelligence and Its Applications*, 2006.

[5] E. Klavins and R. M. Murray, "Distributed Algorithms for Cooperative Control," *IEEE Pervasive Computing*, vol. 3, no. 1, pp. 56–65, Jan-March 2004.

[6] J. Finke, K. M. Passino, and A. Sparks, "Cooperative Control via Task Load Balancing for Networked Uninhabited Autonomous Vehicles," *Proceeding of the IEEE Conference on Decision and Control*, 2003.

[7] R. Olfati-Saber and R. M. Murray, "Consensus Problems in Networks of Agents with Switching Topology and Time-Delays," *IEEE Transactions on Automatic Contol*, vol. 49, no. 9, pp. 1520–1533, September 2004.

[8] T. McLain, P. Chandler, and M. Pachter, "Cooperative Control of UAV Rendezvous," *Proceedings of the American Control Conference*, June 2001.

[9] P. Chandler, S. Rasmussen, and M. Pachter, "UAV Cooperative Path Planning," *Proceedings of AIAA Guidance Navigation and Control Conference*, August 2000.

[10] T. McLain, "Coordinated control of unmanned air vehicles," Air Vehicles Directorate of the Air Force Research Laboratory, Tech. Rep. ASC-99-2426, 1999.

[11] Alphatech Technologies and Products: Dynamic Control of Agent-Based Systems. http://www.alphatech.com/secondary/techpro/task.html.

[12] P. A. Meschler, "Time-Optimal Rendezvous Strategies," *IEEE Transactions on Automatic Control*, vol. 8, no. 3, pp. 279–283, Oct 1963.

[13] J. Arthur E. Bryson and Y.-C. Ho, *Applied Optimal Control*. Taylor & Francis, 1975.

[14] T. McLain, P. Chandler, and M. Pachter, "A Decomposition Strategy for for Optimal Coordination of Unmanned Air Vehicles," *Proceedings of the American Control Conference*, June 2000.

[15] D. Swaroop, "A Method of Cooperative Classification for LOCAAS Vechicles," Air Vehicles Directorate of the Air Force Research Laboratory, Tech. Rep., August 2000.

[16] M. Alighanbari, Y. Kuwata, and J. P. How, "Coordination and Control of Multiple UAVs with Timing Constraints and Loitering," *Proceedings of the American Control Conference*, June 2003.

[17] A. Richards, J. Bellingham, M. Tillerson, , and J. P. How, "Coordination and Control of Multiple UAVs," *Proceedings of the American Control Conference*, June 2003.

[18] H. Khalil, *Nonlinear Systems*. Prentice Hall, 1996.

[19] P. Orgen, M. Egerstedt, and X. Hu, "A Control Lyapunov Function Approach to Multiagent Coordination," *IEEE Transcations on Robotics and Automation*, vol. 18, no. 5, October 2002.

[20] A. Tiwari, J. Fung, J.Carson, R. Bhattacharya, and R. M. Murray, "A Framework for Lyapunov Certificates for Multi-Vehicle Rendezvous Problems," *Proceedings of the American Control Conference*, 2004.

[21] E. D. Sontag, "A 'Universal' Construction of Artstein's Theorem on Nonlinear Stabilisation," *System Control Letters*, vol. 13, no. 2, 1989.

[22] P. Chandler and M. Pachter, "Hierarchical Control for Autonomous Teams," *Proceedings of AIAA Guidance Navigation and Control Conference*, August 2001.

[23] P. R. Chandler, M. Pachter, D. Swaroop, J. M. Fowler, J. K. Howlett, S. Rasmussen, C. Schumacher, and K. Nygard, "Complexity in UAV Cooperative Control," *Proceedings of the American Control Conference*, May 2002.

[24] E. B. Castelan and J. C. Hennet, "On Invariant Polyhedra of Continuous-Time Linear Systems," *IEEE Transactions on Automatic Control*, vol. 38, no. 11, pp. 1680–1685, November 1993.

[25] F. Blanchini, "Set Invariance in Control," *Automatica*, vol. 35, no. 11, pp. 1747–1767, November 1999.

[26] K. Yoshida, H. Kawabe, and Y. Nishimura, "Simple LP-Type Criteria for Positively Invariant Polyhedral Sets," *IEEE Transactions on Automatic Control*, vol. 45, no. 1, pp. 98–101, January 2000.

[27] M. Vassilaki and G. Bitsoris, "Constrained Regulation of Linear Continuous-Time Dynamical Systems," *Systems and Control Letters*, vol. 13, pp. 247–252, 1989.

[28] C. E. T. Dórea and B. E. A. Milani, "Design of L-Q Regulators for State Constrained Continuous-Time Systems," *IEEE Transactions on Automatic Control*, vol. 40, no. 3, pp. 544–548, March 1995.

[29] J. M. da Silva Jr. and S. Tarbouriech, "Invariance and Contractivity of Polyhedra for Linear Continuous-Time Systems with Saturating Controls," *Revista Controle & Automação*, vol. 10, no. 3, pp. 149–156, December 1999.

[30] "A collected scientific papers of paul a. samuelson," J. Stiglitz, Ed. Cambridge, MA: MIT Press, 1966.

[31] D. G. Luenberger, *Introduction to Dynamical Systems*. New York: Wiley.

[32] L. F. Richardson, *Arms and Insecurity*. Pittsburgh, PA: Boxwood Press, Pittsburgh Quadrangle Books.

[33] J. A. Jacquez, *Compartmental Analysis in Biology and Medicine*. New York, NY: Elsevier.

[34] D. H. Anderson, "Compartmental Modelling and Tracer Kinetics," *Lecture Notes in Biomathematics*, 1983.

[35] A. Tiwari, J. Fung, R. Bhattacharya, and R. M. Murray, "Polyhedral Cone Invariance Applied to Rendezvous of Multiple Agents," *Proceeding of the IEEE Conference on Decision and Control*, 2004.

[36] R. A. Horn and C. R. Johnson, *Matrix Analysis*. Cambridge University Press, 1999.

[37] R. Bhattacharya, J. Fung, J.Carson, A. Tiwari, and R. M. Murray, "Ellipsoidal Cones and Rendezvous of Multiple Agents," *Proceedings of the IEEE Conference on Decision and Control*, 2004.

[38] H. Schneider and M. Vidyasagar, "Cross-positive Matrices," *SIAM Journal of Numerical Analysis*, vol. 7, no. 4, November 1970.

[39] J. E. Cohen, "Convexity of the Dominant Eigenvalue of an Essentially Nonnegative Matrix," *Proceedings of the American Mathematical Society*, vol. 81, no. 4, pp. 657–658, April 1981.

[40] C. R. Johnson and D. P. Stanford, "Dominant Eigenvalues Under Trace-Preserving Diagonal Perturbations," *Linear Algebra and its Applications*, vol. 212/213, pp. 415–435, 1994.

[41] R. Bhattacharya, A. Tiwari, J. Fung, and R. M. Murray, "Cone Invariance and Rendezvous of Multiple Agents."

[42] J. Cortes, S. Martinez, T. Karatas, and F. Bullo, "Coverage control for mobile sensing networks," *IEEE Transactions on Automatic Control*, vol. 20, no. 2, pp. 243–255, April 2004.

[43] M. A. Batalin and G. S. Sukhatme, "Sensor coverage using mobile robots and stationary nodes," in *Proceedings of the SPIE*, 2002.

[44] V. Gupta, T. H. Chung, B. Hassibi, and R. M. Murray, "On a stochastic sensor selection algorithm with applications in sensor scheduling and sensor coverage," *Submitted, Automatica*, September 2004.

[45] A. Tiwari, M. Jun, D. E. Jeffcoat, and R. M. Murray, "Analysis of dynamic sensor coverage problem using kalman filters for estimation," in *Proceedings of the 16th IFAC World Congress*, 2005.

[46] B. Sinopoli, L. Schenato, M. Franceschetti, K. Poolla, M. I. Jordan, and S. S. Sastry, "Kalman filtering with intermittent observations," *IEEE Transactions on Automatic Control*, vol. 49, no. 9, pp. 1453–1464, September 2004.

[47] D. E. Jeffcoat, "Coupled detection rates: An introduction," in *Theory and Algorithms for Cooperative Systems*, D. Grundel, R. Murphey, and P. Pardalos, Eds. New Jersey: World Scientific Publishing, 2004, pp. 157–167.

[48] R. A. Horn and C. R. Johnson, *Matrix Analysis*. Cambridge University Press, 1985.

[49] Z. Gajić and M. Qureshi, *Lyapunov Matrix Equation in System Stability and Control*. Academic Press, 1995.

[50] S. Howard, S. Suvorova, and B. Moran, "Optimal policy for scheduling of gauss-markov systems," in *Proceedings of International Conference of Information Fusion*, 2004.

[51] A. Tiwari and R. M. Murray, "Dynamic Sensor Coverage with Uncertainty Feedback: Analysis Using Iterated Maps," *Proceeding of the American Control Conference*, 2006.

[52] F. L. Lewis, *Optimal Estimation with an Introduction to Stochastic Control Theory*. Wiley Interscience, 1986.

[53] A. S. Matveev and A. V. Savkin, *Qualitative Theory of Hybrid Dynamical Systems*. Birkh:auser, 2000.

[54] M. S. Branicky, "Multiple lyapunov functions and other analysis tools for switched and hybrid systems," *IEEE Transactions on Automatic Control*, vol. 43, no. 4, pp. 475–482, April 1998.

[55] R. L. Devaney, *An Introduction to Chaotic Dynamical Systems*. The Benjamin/Cummings Publishing Company, Inc., 1986.

[56] M. Brookes, "The matrix reference manual," *http://www.ee.ic.ac.uk/hp/staff/dmb/matrix/intro.html*, 2005, [online].

[57] A. Graham, *Kronecker Products and Matrix Calculus: with Applications*. John Wiley & Sons, 1981.

[58] N. Yerrick, A. Tiwari, and D. E. Jeffcoat, "An Investigation of a Dynamic Sensor Motion Strategy," *Proceeding of the Conference on Cooperative Control and Optimization*, 2006.

[59] P. Alriksson and A. Rantzer, "Sub-optimal sensor scheduling with error bounds," in *Proceedings of the 16th IFAC World Congress*, 2005.

[60] X. Liu and A. Goldsmith, "Kalman filtering with partial observation losses," 2004.

[61] J. Cortes, S. Martinez, and F. Bullo, "Spatially-distributed coverage optimization and control with limited-range interactions," *ESAIM: Control, Optimization, and Calculus of Variations*, January 2004.

[62] J. S. Rosenthal, "Convergence rates of markov chains," *SIAM Review*, vol. 37, pp. 387–405, 1995.

[63] T. M. Cover and J. A. Thomas, *Elements of Information Theory*. Wiley-Interscience Publication, 1991.

[64] A. Washburn, "Search for a moving target: Upper bound on detection probability," in *Search Theory and Applications*, B. Haley and L. Stone, Eds. New York, NY: Plenum Press, 1980, pp. 231–237.

[65] L. Stone, *Theory of Optimal Search*, 2nd ed. Operations Research Society of America, 1989.

[66] R. A. Horn and C. R.Johnson, *Matrix Analysis*. Cambridge University Press, 1985.

[67] P. Lancaster and L. Rodman, *Algebraic Riccati Equations*. Clarendon Press, Oxford, 1995.

[68] B. D. O. Anderson and J. B. Moore, *Optimal Filtering*. Prentice-Hall Inc., 1979.

[69] P. d'Alessandro and E. D. Santis, "Controlled Invariance and Feedback Laws," *IEEE Transactions on Automatic Control*, vol. 46, no. 7, pp. 1141–1146, July 2001.

[70] E. B. Castelan and J. C. Hennet, "Eigenstructure Assignment for State Constrained Linear Continuous Time Systems," *Automatica*, vol. 28, no. 3, pp. 605–611, 1992.

[71] A. Berman, M. Neumann, and R. J. Stern, *Nonnegative Matrices in Dynamic Systems*. Wiley-Interscience, 1989.

[72] J. P. LaSalle, "The Time Optimal Control Problem," *Contributions to the Theory of Nonlinear Oscillations*, vol. 5, 1960.

[73] L. W. Neustadt, "Synthesizing Time Optimal Control Systems," *Journal of Mathematical Analysis and Applications*, vol. 1, pp. 484–493, 1960.

[74] M. B. Milam, K. Mushambi, and R. M. Murray, "A New Computational Approach to Real-Time Trajectory Generation for Constrained Mechanical Systems," *Proceedings of the IEEE Conference on Decision and Control*, 2000.